DEMOCRATIC AND POPULAR REPUBLIC OF ALGERIA
MINISTRY OF HIGH EDUCATION AND SCIENTIFIC RESEARCH
UNIVERSITY OF MOHAMED BOUDIAF - M'SILA

FACULTY OF SCIENCES
DEPARTMENT OF PHYSICS

N° : PH/MAT/10/2025

DOMAINE: SCIENCE OF MATTER
FIELD : PHYSICS
OPTION : MATERIAL PHYSICS

Memory Submitted for Obtaining
Diploma of Academic Master

By:

Douidi ali aboubakeur

TITLE

Study of the mechanical and thermodynamic properties of some MAX phase compounds using computational methods

Defended on 18/06/2025 in front of a jury composed of:

Allali djamel	**University of Msila**	**Chairman**
Saber Saad Essaoud	**University of Msila**	**Supervisor**
Karim boufferrache	**University of Msila**	**Examiner**

Academic Year: 2024/2025

شكر
وتقدير

الحمد لله عدد ما كان وعدد ما يكون، وعدد الحركات والسكون، الحمد لله الذي علم الإنسان ما لم يعلم، وسخّر له من النعم ما لا يُعدّ ولا يُحصى .
الحمد لله الذي أكرمنا بالعقل وهدانا لنور العلم، وجعل لنا من القرآن الكريم هدىً وشفاء، وأرسل لنا خير خلقه محمدًا ﷺ رحمة للعالمين، فصلى الله عليه وسلم عدد ما ذكره الذاكرون وغفل عن ذكره الغافلون .

نحمده ونشكره أن أتمّ علينا هذه النعمة، ووفقنا في هذا المشوار العلمي الطويل، الذي لم يكن سهلًا، ولكن بعون الله وصبرنا وإصرارنا استطعنا أن نصل إلى هذه اللحظة .

ونتوجه بخالص الشكر والعرفان لكل من وضع في طريقنا حرفًا علّمنا به، ولكل معلم أفاض بعلمه وساهم في بناء معرفتنا، منذ الخطوة الأولى في مسيرتنا التعليمية وحتى هذه اللحظة المميزة ..

شكر خاص وعميق نرفعه إلى مشرفنا الكريم الدكتور صابر سعد السعود، على دعمه المستمر وتوجيهاته القيّمة، التي كانت نبراسًا لنا طوال فترة إعداد هذا العمل. كما لا يفوتنا أن نشكر أعضاء لجنة المناقشة الكرام، الأستاذ علالي جمال والأستاذ بوفراش كريم، على تفضلهم بتقييم هذا الجهد المتواضع.

وفي الختام، نسأل الله أن يبارك في علمنا وعملنا، ويجعله خالصًا لوجهه الكريم، وأن يرزقنا القبول والتوفيق، والعافية في الدين والدنيا، إنه وليّ ذلك والقادر عليه

علي ابوبكر

إهداء

الحمد لله، والصلاة والسلام على سيدنا محمد، النبي المصطفى، وعلى آله وصحبه أجمعين.

إلى من وهبه الله الهيبة والوقار، ومن غرس في قلبي معنى الرجولة والاحترام...

إلى من أعتز بحمل اسمه وأفتخر به في كل محفل ومكان...

إلى والدي الغالي "عبد الدائم" – رحمه الله رحمة واسعة، وغفر له، وأسكنه فسيح جناته، وجعل قبره روضة من رياض الجنة.

وإلى من كانت رحمة وحنانًا تمشي على الأرض، إلى من ربّتني بحبها، وسهرت لأجلي، وكانت حضنًا دافئًا لا يُنسى...

إلى والدتي العزيزة "زينب" – رحمها الله وأسكنها الفردوس الأعلى، وجعل دعائي لها نورًا في قبرها ورحمة لا تنقطع.

وإلى من كان قدوتي في الأخلاق والعلم والرقي، أستاذي الفاضل "صابر سعد السعود" – جزاه الله عني خير الجزاء، وبارك في عمره، وزاده من فضله وعلمه.

وإلى زوجتي ، رفيقة دربي ، التي وقفت بجانبي في كل لحظة، وكانت لي دعمًا وأمانًا، فشكرًا لها من القلب، وجزاها الله عني كل خير

وإلى أولادي الأعزاء، زينة حياتي ونور عيوني، من أجلهم أعمل وأسعى، وأسأل الله أن يبارك فيهم، ويحفظهم من كل شر، ويجعلهم من عباد الله الصالحين.

وإلى عائلتي الكريمة، التي كانت ولا تزال سندي ودعمي في كل خطوة، لكم مني كل الحب والتقدير

ولا أنسى أصدقائي وزملائي الذين شاركوني هذه الرحلة، وكانوا جزءًا من هذا النجاح، فلكم مني كل الشكر والدعاء والتقدير

Table of Contents

Table of Contents	
Thanks and gratitude	
Dedication	
List of figures	
List of tables	
General introduction	01
CHAPTER 1: THEORETICAL PART	
1- The Schrödinger Equation	06
2- Born-Oppenheimer Approximation	07
3- Hartree and Hartree-Fock Approximations (HF)	08
4- Density Functional Theory (DFT)	10
4-1 Formalism of Density Functional Theory (DFT)	12
I. Hohenburg and Kohn Theorems	12
II. The Kohn - Sham equation	13
B-1) Solution of the Kohn - Sham Equation	15
5-The Different Types of Approximation of the Excρ	19
5-1 Local density approximation (LSDA)	19
5-2 The Generalized Gradient Approximation GGA	19
5-3 The mBJ Approximation (modified Becke–Johnson)	20
6- Full-Potential Linearized Augmented Plane-wave Method (FP-LAPW)	20
6-1 The Plane Wave method (APW)	20
6-2 The Linearized Augmented Plane Wave Method (LAPW)	22
7- WIEN2K software	23
8-References	26
CHAPTER 2: RESULTS AND DISCUSSION	
1- Introduction	29
2- Calculation Details	29
3- Results and discussion	30
3-1 Structural properties	30
3-2 Electronic Properties	34
3-2-1 Energy Bands	34
3-2-2 Total Density of States (TDOS) Partial Density of States (PDOS)	36
4- The Thermodynamic Properties	39
4-1 Heat Capacities	40
4-2 Entropy	42
4-3 Thermal Expansion Coefficien	43

4-4 The Debye temperature	45
5-The elastic Properties	47
References	50
Conclusion	51

List of figures

CHAPTER 1	
FIGURE (I-1): Self-consistent calculation flowchart	18
FIGURE (I-2): Diagram of the distribution of the elementary cell in atomic spheres and in interstitial region	20
FIGURE (I-3): The flowchart of the Wien2k code subroutines	25
CHAPTER 2	
FIGURE (II-1): Crystal structure of V2SnC and V2SnN compounds	30
FIGURE (II-2) : Total Energy-Volume and volume-pressure Curves of V_2SnN calculated using GGA-sol approximations.	32
FIGURE (II-3): Total Energy-Volume and volume-pressure Curvesof V_2SnC calculated using GGA-sol approximations	33
FIGURE (II-4): The hexagonal Brillouin zone	
FIGURE (II-5): band structure spectra for both compounds V_2SnC and V_2SnN	35
FIGURE (II-6): Total and partial density of states of V_2SnN	37
FIGURE (II-7): Total and partial density of states of V_2SnC	38
FIGURE (II-8): variation of the heat capacity "Cv" of the compound V_2SnC as a function of temperature	41
FIGURE (II-9): variation of the heat capacity "Cv" of the compound V_2SnN as a function of temperature	41
. **FIGURE (II-10):** variation of the entropy (S) as function of temperature of V_2SnC	42
FIGURE (II-11): variation of the entropy (S) as function of temperature of V_2SnN	43
FIGURE (II-12): variation of the thermal expansion coefficient (α) as function of temperature of V_2SnC	44
FIGURE (II-13): variation of the thermal expansion coefficient (α) as function of temperature of V_2SnN	44
FIGURE (II-14): variation of The Debye temperature θD as function of temperature of V_2SnC	45
FIGURE (II-15): variation of The Debye temperature θD as function of temperature of V_2SnN	46

List of Tables

CHAPTER 1	
TABLE (I-1): Comparison between the two methods, Hartree-Fock and the Density Functional Theory (DFT)	09
CHAPTER 2	
TABLE (II-1) : Atomic positions for V_2SnC and V_2SnN compounds	30
TABLE (II-2) : Values of the structural parameters obained for V2SnC and V2SnN compounds and calculated by GGA approximation	32
TABLE (II-3) : Elastic constants (C_{ij}), Young's modulus Y, Poisson's ration (υ), Anisotropy(A), Bulk (B) and Shear modulus (G), G/B ratio, f-index , ductility U_d and machinability U_M factors of M_2AX phases (M= V , A= Sn, X = C or N)	49

INTRODUCTION

Introduction

The term "MAX phase materials" was first use d in 2000 by Barsoum [1]. These materials consist of three different types of atoms: transition metal M, atoms from the A group, and C or N atoms. All of these atoms crystallize in a hexagonal structure with the chemical formula $M_{n+1}AX_n$ (n=1-3).

MAX phase compounds offer high elastic moduli, high-temperature mechanical capabilities, and corrosion and oxidation resistance by combining ceramic and metallic features. They are also resistant to thermal shock, deformable at ambient temperature, and have high electrical and thermal conductivities. Because of these characteristics, they are promising and often used materials that, when heated, can compensate for graphite's resistance to high temperatures.

Numerous theoretical and practical investigations of this kind of material have recently demonstrated that certain of them only exhibit superconductivity for ternary carbides M_2AC, where M stands for Ti, Nb, and Mo and A for S, Ga, As, In, and Sn [2]. Bouhemadou et al. conducted a theoretical study on the structural and elastic properties of Nb2InC M2InC phases and M2GaC, with M= Ti, V, Nb, and Ta, under pressure effect, in addition to numerous other works that deal with determining the elastic properties of other materials for this type [3,4]. Scabarozi *et al.* [5] were measured the linear thermal expansion coefficient by high-temperature X-ray diffraction and dilatometry of some MAX phase materials. Jonathan *et al.* [6] have also studied the three compounds Ti_2AlC, Ti_3AlC_2, and Ti_3SiC_2 and calculated their resistivity, in order to use them as surfaces for electrocatalyst support materials in hydrogen fuel cells. Experimentally, Carlos et al. [7] have prepared the MAX phases Ti_2AlC and Ti_3AlC_2 as thin films in high purity via thermal treatment and analyzed them using both XRD and Raman spectroscopy, several properties such as the hardness and the elastic modulus for both MAX phases have been evaluated using nano-indentation tests.

Further characteristics of ceramic-metallic materials have been investigated and addressed, particularly the most recent study on how stress affects the magnetic properties of Mn_2AlC and Mn_2SiC compounds [8] as well as the study of Superconducting phases in a class of metallic ceramics and other properties in many studies carried out by Hadi et al [9–11].

This thesis is organized as follow :

- The first chapter provides a theoretical overview of studying any crystalline system based on Density Functional Theory (DFT) [12–17] , Hartree-Fock (HF) approximation, as well as the GGA and mBJ approximations to solve the Schrödinger equation.
- The second chapter applies the concepts discussed in the first chapter using the Wien2K program to calculate the structural properties, employing the GGA-PBEsol approximation for compounds **V_2SnC** and **V_2SnN**. This includes parameters such as lattice constant (a), bulk modulus (B), and a study of their magnetic and electronic behavior. The electronic behavior of both **V_2SnC** and **V_2SnN** compounds was also verified, and we calculated the elastic properties such as elastic constants, bulk modulus, shear modulus, Young's modulus, and mechanical stability of the two compounds. Finally, the effect of both temperature and pressure on the thermal properties of the compounds was studied.

References

[1] M.W. Barsoum, The MN+ 1AXN phases: A new class of solids: Thermodynamically stable nanolaminates, Prog. Solid State Chem. 28 (2000) 201–281.

[2] D. Music, J.M. Schneider, The correlation between the electronic structure and elastic properties of nanolaminates, Jom 59 (2007) 60–64.

[3] Y. Medkour, A. Bouhemadou, A. Roumili, Structural and electronic properties of M2InC (M= Ti, Zr, and Hf), Solid State Commun. 148 (2008) 459–463.

[4] A. Bouhemadou, R. Khenata, Prediction study of structural and elastic properties under the pressure effect of M 2 GaC (M= Ti, V, Nb, Ta), J. Appl. Phys. 102 (2007) 043528.

[5] T.H. Scabarozi, S. Amini, O. Leaffer, A. Ganguly, S. Gupta, W. Tambussi, S. Clipper, l J. Spanier, M.W. Barsoum, J.D. Hettinger, Thermal expansion of select M n+ 1 AX n (M= early transition metal, A= A group element, X= C or N) phases measured by high temperature x-ray diffraction and dilatometry, J. Appl. Phys. 105 (2009) 013543.

[6] J. Gertzen, P. Levecque, T. Rampai, T. van Heerden, DFT Study of MAX Phase Surfaces for Electrocatalyst Support Materials in Hydrogen Fuel Cells, Materials 14 (2021) 77.

[7] C. Torres, R. Quispe, N.Z. Calderón, L. Eggert, M. Hopfeld, C. Rojas, M.K. Camargo, A. Bund, P. Schaaf, R. Grieseler, Development of the phase composition and the properties of Ti2AlC and Ti3AlC2 MAX-phase thin films–A multilayer approach towards high phase purity, Appl. Surf. Sci. 537 (2021) 147864.

[8] A. Azzouz-Rached, M.A. Hadi, H. Rached, T. Hadji, D. Rached, A. Bouhemadou, Pressure effects on the structural, elastic, magnetic and thermodynamic properties of Mn2AlC and Mn2SiC MAX phases, J. Alloys Compd. 885 (2021) 160998.

[9] M.A. Hadi, N. Kelaidis, S.H. Naqib, A. Islam, A. Chroneos, R.V. Vovk, Insights into the physical properties of a new 211 MAX phase Nb2CuC, J. Phys. Chem. Solids 149 (2021) 109759.

[10] M.A. Hadi, Superconducting phases in a remarkable class of metallic ceramics, J. Phys. Chem. Solids 138 (2020) 109275.

[11] M.A. Hadi, N. Kelaidis, S.H. Naqib, A. Islam, A. Chroneos, R.V. Vovk, Insights into the physical properties of a new 211 MAX phase Nb2CuC, J. Phys. Chem. Solids 149 (2021) 109759.

[12] A. Görling, Density-functional theory beyond the Hohenberg-Kohn theorem, Phys. Rev. A 59 (1999) 3359–3374. https://doi.org/10.1103/physreva.59.3359.

[13] P. Hohenberg, W. Kohn, Inhomogeneous Electron Gas, Phys. Rev. 136 (1964) B864–B871. https://doi.org/10.1103/physrev.136.b864.

[14] Á. Nagy, Density functional. Theory and application to atoms and molecules, Phys. Rep. 298 (1998) 1–79. https://doi.org/10.1016/s0370-1573(97)00083-5.

[15] B.T. Sutcliffe, The Fundamentals of Electron Density, Density Matrix and Density Functional Theory for Atoms, Molecules and the Solid State — A Forum Preview, Fundam. Electron Density Density Matrix Density Funct. Theory At. Mol. Solid State (2003) 3–8. https://doi.org/10.1007/978-94-017-0409-0_1.

[16] R.G. Parr, Density Functional Theory of Atoms and Molecules, Horiz. Quantum Chem. (1980) 5–15. https://doi.org/10.1007/978-94-009-9027-2_2.

[17] T.A. Wesołowski, Hohenberg-Kohn-Sham Density Functional Theory, Chall. Adv. Comput. Chem. Phys. (n.d.) 153–201. https://doi.org/10.1007/1-4020-5372-x_2.

CHAPTER 1 :

THEORETICAL STUDY

CHAPTER 1:

THEORETICAL PART

Table of Contents

Table of Contents 5
1- The Schrödinger Equation 6
2- Born-Oppenheimer Approximation 7
3- Hartree and Hartree-Fock Approximations (HF) 8
4- Density Functional Theory (DFT) 10
4-1 Formalism of Density Functional Theory (DFT) 12
I. Hohenburg and Kohn Theorems 12
II. The Kohn - Sham equation 13
B-1) Solution of the Kohn - Sham Equation 15
5-The Different Types of Approximation of the Excρ 19
5-1 Local density approximation (LSDA) 19
5-2 The Generalized Gradient Approximation GGA 19
6- Full-Potential Linearized Augmented Plane-wave Method FP-LAPW 20
6-1 The Plane Wave method (APW) 20
6-2 The Linearized Augmented Plane Wave Method (FP-LAPW) 22
7-WIEN2K software 23
8- References …. 26

1- The Schrödinger Equation

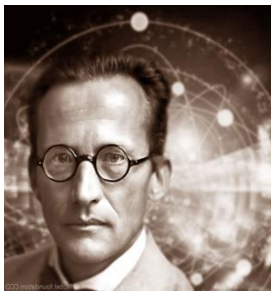

The Schrödinger equation was formulated in 1926 by the Austrian scientist Erwin Schrodinger (1887-1961) [1] ، who shared the Nobel Prize for Physics with Paul Dirac in 1933 for their outstanding contribution to quantum physics. This equation is the cornerstone of quantum mechanics, which specializes in the study of systems involving microscopic particles. Schrödinger built on the ideas of a number of scientists such as Planck and De Broglie, who were interested in studying the system consisting of nuclei and moving electrons as these particles exchange influence with each other through their wave function, which carries all the necessary information about the studied system[2,3] The Schrödinger equation has the following expression :

$$H\Psi(\vec{R}_I, \vec{r}_i) = E\Psi(\vec{R}_I, \vec{r}_i) \quad \text{(I.1)}$$

The two vectors $\vec{R}_I$ and $\vec{r}_i$ are the coordinates of the nucleus (I) and of the electron (i).

H: Hamiltonian operator related to the sum of the kinetic energy and the potential energy of the system.

E: eigenvalue Energy of the system.

Ψ: wave function which depends on the coordinates of electrons and nuclei.

The Hamiltonian system - made up of nuclei and electrons - includes the kinetic energy of electrons and nuclei, as well as the potential energies (electron-electron, electron-nucleus, and nucleus-nucleus), therefore the expression of the total Hamiltonian of the system is written by the following expression:

$$H = T_e + T_N + V_{ee} + V_{e-N} + V_{N-N} \quad \text{(I.2)}$$

$T_e = -\sum_i \frac{\hbar^2}{2m_i} \vec{\nabla}_i^2$ →Electronic kinetic energy (m_i the mass of electron i).

$T_n = -\sum_I \frac{\hbar^2}{2m_I} \vec{\nabla}_I^2$ →Nuclei kinetic energy (m_I the mass of the nucleus I).

$V_{N-N} = \sum_{I \neq J} \frac{Z_I Z_J e^2}{|R_I - R_J|}$ →The interaction part between the nuclei.

$V_{e-N} = \sum_{I,j} \frac{Z_I e^2}{|R_I - r_j|}$ →The nuclei-electrons interaction part.

$V_{e-e} = \sum_{i \neq j} \frac{e^2}{|r_i - r_j|}$ →The interaction part between the electrons.

$|R_\alpha - R_\beta|$ → The distance between the two nuclei α and β

$|r_i - R_\alpha|$ → The distance between the nucleus α and the electron i

$|r_i - r_j|$ → The distance between the two electrons i and j.

solving the Schrödinger equation can be really hard, especially for systems with lots of electrons and moving parts, and their complicated interactions. So, scientists use simpler methods to get close to the right answer. Here are some of the main ways they do that:

2- Born-Oppenheimer Approximation

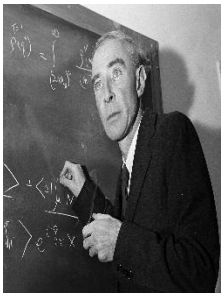

The Born-Oppenheimer approximation was proposed by scientists Max Born and Robert Oppenheimer in 1927[4], it is one of the basic concepts underlying the description of the quantum states of molecules .This approximation is based on the idea of separating the study of the motion of nuclei from the motion of electrons, that is, adopting independence in the study without the need to consider the interaction between them.This approximation makes it possible to separate the motion of the nuclei and the motion of the electrons. due to the large difference in mass between electrons and nuclei. Consequently, the nucleus, relative to the electrons, can be assumed to be at rest, allowing the motion of the nuclei to be ignored and the nucleus-nucleus interaction energy to be considered as a constant quantity (V_{nn} = Constant).

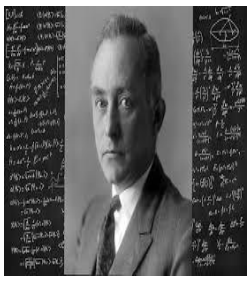

The Born-Oppenheimer approximation was applied to the Schrödinger equation, resulting in significant progress in solving the equation. The most notable results were as follows :

According to the Born-Oppenheimer approximation we can rewrite the total wave function of the system $\Psi\left(\vec{R}_I^{\,0}, \vec{r}_i\right)$ in the form of a product of an electronic function $\Psi_e\left(\vec{R}_I^{\,0}, \vec{r}_i\right)$ and a nuclear function $\Psi_n\left(\vec{R}_I^{\,0}\right)$, thus, we can separate the motion of nuclei from that of electrons. Then the wave function is written:

$$\Psi\left(\vec{R_I}^{\,0},\vec{r_i}\right)=\Psi_n\left(\vec{R_I}^{\,0}\right)\Psi_e\left(\vec{R_I}^{\,0},\vec{r_i}\right) \quad \text{(I.3)}$$

$$\begin{cases}[T_e\ +V_{ee}+V_{en}]\Psi_e\left(\vec{R}_{\mathrm{I}}^{\,0},\vec{r}_{\mathrm{i}}\right)=E_e\left(\vec{R}_{\mathrm{I}}^{\,0}\right)\Psi_e\left(\vec{R}_{\mathrm{I}}^{\,0},\vec{r}_{\mathrm{i}}\right)\\ \left[T_n+V_{nn}+E_e\left(\vec{R}_{\mathrm{I}}^{\,0}\right)\right]\Psi_n\left(\vec{R}_{\mathrm{I}}^{\,0}\right)\ =E\Psi_n\left(\vec{R}_{\mathrm{I}}^{\,0}\right)\end{cases} \quad \text{(I.4)}$$

Despite the use of Born-Oppenheimer simplifications in the Schrödinger equation, the electron-electron interaction remains a complex challenge that hinders efforts to solve the equation. Due to this complexity, the equation remains a challenge to solve using standard mathematical methods, prompting scientists to resort to other approximations to facilitate its solution

3- Hartree and Hartree-Fock Approximations (HF)

Scientist Hartree introduced a new approximation to the Schrödinger equation in 1928 [5–7]after the Born-Oppenheimer approximation. This approximation is based on the principle of independent particles,[8,9] .In this approximation, Hartree treats the interactions between electrons as particles carrying a charge without taking into account the spin state, i.e. The interactions are simplified to Coulombic repulsion interactions, overlooking both exchange and correlation terms. Additionally, the wave function lacks "anti-symmetry" as it does not account for the Pauli exclusion principle. [3,10].

Although the Hartree approximation overlooks electron spin and the Pauli exclusion principle, it simplifies the Schrödinger equation by reducing the study of a large number of electrons to that of a single electron., so that the total Hamiltonian H of electrons is the sum of the Hamiltonians hi of each electron, while the total wave function of the electronic system represents by multiplication the individual wave functions of each electron [3,10].

Finally,the total energy of the electronic system is the aggregate of the energies of all electrons. Following Hartree's approximation, the Hamiltonian equation for a single electron can be expressed as follows:

$$H = \sum_i h_i \quad \text{(I.5)}$$

$$h_i = -\frac{\hbar^2}{2m_i}\Delta_i - \sum_I \frac{Z_I e^2}{\left|\vec{r_i} - \vec{R_I}^0\right|} + \frac{1}{2}\sum_j \frac{e^2}{|\vec{r_i} - \vec{r_j}|} \quad \text{(I.6)}$$

$$\Psi_e = \prod_i \Psi_i \quad \text{(I.7)}$$

$$E_e = \sum_i \varepsilon_i \quad \text{(I.8)}$$

In 1930, Fock [9] improved and refined Hartree's model by replacing electron wave functions with a Slater determinant[10]. This change allowed Fock to address the exchange effect, which Hartree had overlooked. As a result, the interaction between electrons now includes both Coulomb interaction and the exchange effect. This led to the replacement of previous functions with anti-symmetric functions. In his analysis of electronic interactions, Fock introduced the concept of "spin" and replaced the electronic system's wave function with a Slater determinant, as expressed by the formula:

$$\Psi_{HF}(\vec{r}_1, \vec{r}_2, \vec{r}_3, \dots, \vec{r}_N) = \frac{1}{\sqrt{N_e!}} \begin{bmatrix} \psi_1(\vec{r}_1) & \psi_1(\vec{r}_2) & \psi_1(\vec{r}_3) & \cdots & \psi_1(\vec{r}_N) \\ \psi_2(\vec{r}_1) & \psi_2(\vec{r}_2) & \psi_2(\vec{r}_3) & \cdots & \psi_2(\vec{r}_N) \\ \psi_3(\vec{r}_1) & \psi_3(\vec{r}_2) & \psi_3(\vec{r}_3) & \dots & \psi_3(\vec{r}_N) \\ \vdots & \vdots & \vdots & \ddots & \vdots \\ \psi_N(\vec{r}_1) & \psi_N(\vec{r}_2) & \psi_N(\vec{r}_3) & \cdots & \psi_N(\vec{r}_N) \end{bmatrix} \quad \text{(I.9)}$$

where $\frac{1}{\sqrt{N_e!}}$is a normalization factor.

Despite the positive achievements of the Hartree-Fock approximation, it remains unable to solve the challenge of quantum correlation between electrons, which involves quantum interaction. In addition, the Schrödinger equation continues to present analytical challenges. For this reason, subsequent studies after Hartree-Fock's work were directed towards the search for simpler and more accurate theories in terms of results, epitomized by density functional theory (DFT).

4- Density Functional Theory (DFT)

Density Functional Theory (DFT) is characterized by an attempt to provide a more simplified formulation of the Schrödinger equation that describes the motion of electrons. This is done by using electron density instead of wave functions to express the kinetic energies and interactions between electrons. The density functional theory was developed in 1927 by scientists Thomas and Fermi[13,14] ‘, who analogized the electronic system to a homogeneous and uniform electron gas. As a result of this approach, two mathematical relationships were arrived at that express the density and kinetic energy of a homogeneous electron gas sequentially:

$$\rho = \frac{1}{3\pi^2} E_f^{\frac{3}{2}} \left(\frac{2m_e}{h^2}\right)^{\frac{3}{2}} \qquad \text{(I.10)}$$

$$E_c = \frac{3}{5}\left(\frac{h^2}{2m_e}\right)(3\pi^2)^{\frac{2}{3}}\rho^{\frac{5}{2}} \qquad \text{(I.11)}$$

The theoretical work of scientists such as Lederach, Slater, Hohenberg and Kuhn[12] has contributed to the advancement of density function theory, and these efforts have yielded results that closely approximate experimental results.

HF method	DFT
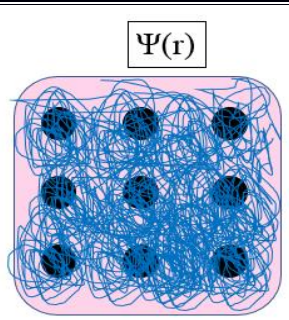	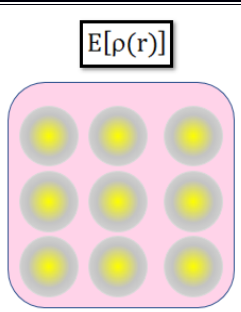
• Principle: Schrödinger equation is solved by considering the wave functions as a variable basic. • Depended on the theory of the mean field theory (MFT). • Calculates wave functions and eigenvalue energy to obtain ground state energy. • Depend on the large number of variables, which makes the equation very complicated and time consuming. • The wave functions obtained as solutions for the Schrödinger equation have no physical meaning. • Does not take into account the correlation terms.	• Principle: Solving the Schrödinger equation by considering the electron density as a variable basic. • Based on the two Hohenburg – Sham theorems and shifting from the Schrödinger equation to the Kohn-Sham equations to find the solution. • Use electron density which has physical meaning. • Reduce the number of variables which makes the equation simpler and faster compared to the HF method. • Used to treat the correlation terms.

TABLE (I. 1): Comparison between the two methods, Hartree-Fock and the Density Functional Theory (DFT)[14,15].

4-1 Formalism of Density Functional Theory (DFT)

Density Functional Theory (DFT) is based on the principle of representing the total energy of a system comprising multiple interacting electrons in terms of the electronic density instead of the wave function. The electronic density is mathematically defined by the following equation:

$$\rho(\vec{r}) = \sum_{i=1}^{N} |\Psi_i(\vec{r})|^2 \qquad \text{(I.12)}$$

This approach simplifies the problem by focusing on the spatial distribution of electrons rather than dealing with the complexity of the many-electron wave function.

I. Hohenburg and Kohn Theorems :

The foundation of Density Functional Theory (DFT) is based on two fundamental theorems introduced by Hohenberg and Kohn. These theorems establish that the total energy of an electronic system within an external potential $V(\vec{r})$ can be expressed as a functional of the electronic density. By determining this density, all properties of the system can be derived:

$$E[\rho(\vec{r})] = F[\rho(\vec{r})] + \int V(\vec{r})\rho(\vec{r})dr^3 \qquad \text{(I.13)}$$

Here $F[\rho(\vec{r})]$ is a universal functional of the electronic density that accounts for the contributions of the kinetic energy and the electron-electron interactions [10,15]. This functional is mathematically represented to describe how different energy contributions, such as kinetic energy and electron interactions, are incorporated into the overall electronic density of the system:

$$F[\rho] = T[\rho] + U[\rho] \qquad \text{(I.14)}$$

The external potential generated by the nuclei is expressed as:

$$V_{ext}(\vec{r_i}) = -\sum_A \frac{Z_A}{r_{iA}} \qquad \text{(I.15)}$$

in the context of Density Functional Theory specifies the conditions for obtaining the total energy of the electronic system in its ground state. This is achieved by identifying the electronic density that minimizes the energy functional, ensuring that the energy functional reaches its lowest value:

$$E(\rho_0(\vec{r})) \leq \mathrm{E}\,[\rho(\vec{r})] \quad \text{(I.16)}$$

$$E(\rho_0) = MinE(\rho) \lim_{\rho \to N} \langle \Psi | \hat{T} + \sum_i V_{ext} + V_{ee} | \Psi \rangle \quad \text{(I.17)}$$

To find the electronic density corresponding to the ground state, the principle of variation is used [16] . This principle involves differentiating the total energy with respect to the electronic density and applying the following mathematical relationship, which depends on the universal functional F[ρ(r⃗)]and the external potential V(r)[10] .

$$\frac{d\mathrm{F}\,[\rho(\mathrm{r})]}{d\rho(\mathrm{r})} + \mathrm{V}(\mathrm{r}) = 0 \quad \text{(I.18)}$$

II. The Kohn - Sham equation:

One of the primary challenges in studying many-electron systems is the difficulty in analytically expressing the kinetic energy and electron-electron interactions as functions of the electron density. In 1965, Kohn and Sham introduced a revolutionary approach to address this issue.

They proposed replacing the real electronic system with a fictitious system in which electrons are considered to move independently, unaffected by one another, except through an effective potential. This effective potential, known as the Kohn-Sham potential, accounts for both the external potential generated by the nuclei and the potential arising from interactions with the other electrons in the system [3,17,18].

The Kohn-Sham fictitious system is defined by the following principles:

Kohn-Sham orbitals: These are single-electron wavefunctions that are solutions of the Schrödinger equation in this independent-electron framework.

Density equivalence: The fictitious system is constructed to ensure that its electronic density matches that of the real system.

Kinetic energy decomposition: The kinetic energy of the fictitious system T_f represents the kinetic energy of non-interacting electrons, while the kinetic energy of the real system

T_R is expressed as the sum of T_f and a correction term T_c that accounts for correlation effects[3]:

$$T_R = T_f + T_c \qquad \text{(I.19)}$$

$$T_c = \langle \Psi | T | \Psi \rangle - \langle \varphi | T_s | \varphi \rangle \qquad \text{(I.20)}$$

Additionally, the electron-electron interaction energy in the real system (V_{ee}) is decomposed as:

$$\langle \Psi | V_{ee} | \Psi \rangle = U_H + U_x + U_c \qquad \text{(I.21)}$$

where:

U_H: The electronic Coulomb (Hartree potential)

U_x: The exchange energy.

Uc: The correlation energy between the electrons.

Components of the Kohn-Sham Equation

The Kohn-Sham equation for an electronic system is derived by considering contributions from the kinetic energy, the external potential, the Hartree interaction, and the exchange-correlation energy. The terms are detailed as follows:

- -Kinetic energy of the fictitious system:

$$T_s[\rho] = \left\langle \varphi_i \middle| -\frac{\hbar^2}{2\mathrm{m}} \Delta \middle| \varphi_i \right\rangle = -\frac{\hbar^2}{2\mathrm{m}} \sum_{\mathrm{i}} \int \varphi_i \nabla^2 \varphi_i^* dr_i \qquad \text{(I.22)}$$

- External potential (nucleus-electron interaction):

$$V_{NE}[\rho] = -\int \sum_{I,i} \frac{Z_I \rho(\vec{r})}{\left| \vec{R}_{\mathrm{I}}^{\,0} - \vec{r} \right|} dr \qquad \text{(I.23)}$$

- 3-Hartree potential (electron-electron Coulomb interaction):

$$U[\rho] = \frac{1}{2} \int \frac{\rho(\vec{r}) \rho\left(\overrightarrow{r'}\right)}{\left| \vec{r} - \overrightarrow{r'} \right|} dr dr' \qquad \text{(I.24)}$$

- 4-Exchange-correlation energy:

The exchange-correlation energy is the sum of the exchange (E_x) and correlation (E_c) contributions. While its exact expression is unknown, it is approximated in practical calculations:

$$E_{xc}[\rho] = E_x[\rho] + E_c[\rho] \qquad \text{(I.25)}$$

The Kohn-Sham equation is finally expressed as[19–21]:

$$H_{KS}\varphi_i(\vec{r}) = [T_s[\rho] + V_{KS}(\vec{r})]\varphi_i(\vec{r}) = \varepsilon^{KS}\varphi_i(\vec{r}) \qquad \text{(I.26)}$$

where the Kohn-Sham potential $V_{KS}(\vec{r})$ includes contributions from:

$$V_{KS}(\vec{r}) = V_{ext}(\vec{r}) + V_H(\vec{r}) + +V_{XC}(\vec{r}) \qquad \text{(I.27)}$$

The total energy of the system is given by:

$$E[\rho] = T_s[\rho] + V_{NE}[\rho] + U_H[\rho] + E_{xc}[\rho] \qquad \text{(I.28)}$$

B-1) Solution of the Kohn - Sham Equation

The solution of the Kohn-Sham equation involves two fundamental steps:

- **Defining the terms of the effective Kohn-Sham potential**:

A critical aspect of this step is determining the exchange-correlation potential,E_{xc} . Unlike other components of the Kohn-Sham potential, E_{xc} does not have a closed-form analytical expression and must instead be approximated using suitable models or computational techniques.

- **Finding the wave functions (Kohn-Sham orbitals):**

The Kohn-Sham orbitals,

represent the solutions to the Kohn-Sham equation and can be expressed as a linear combination of basis functions[3]:

$$\varphi_{KS}(\vec{r}) = \sum_j C_{ij}\,\varphi_j(\vec{r}) \qquad \text{(I.29)}$$

Here, $\varphi_{KS}(\vec{r})$ are the basis functions, and C_{ij} are the expansion coefficients. The equation is solved in the form:

$$\sum_j C_{ij} H_{KS}|\varphi_j\rangle = \sum_j C_{ij}\varepsilon_{KS}|\varphi_j\rangle \qquad \text{(I.30)}$$

$$\langle\varphi_k|\sum_j C_{ij} H_{KS}|\varphi_j\rangle = \langle\varphi_k|\sum_j C_{ij}\varepsilon_{KS}|\varphi_j\rangle \qquad \text{(I.31)}$$

By projecting onto the basis set, the equation can be reformulated as:

$$\sum_j \quad (\langle\varphi_k|H_{KS}|\varphi_j\rangle - \varepsilon_{KS}\langle\varphi_k|\varphi_j\rangle)C_{ij} = 0 \qquad \text{(I.32)}$$

The solution requires determining the expansion coefficients C_{ij}

- **Iterative Solution Procedure**

The Kohn-Sham equation is solved iteratively using the self-consistent field (SCF) method. The process is illustrated in Figure (1.I) and proceeds as follows:

- Initialization:

Begin with an initial guess for the electron density, ρ_{in}, typically derived from a superposition of atomic densities.

- Constructing the Kohn-Sham matrix:

Using the initial density, solve the Kohn-Sham equation to compute the Kohn-Sham orbitals, $\varphi_{KS}(\vec{r})$, and calculate the Kohn-Sham Hamiltonian matrix elements.

- Calculating the new density:

Compute the new electron density, ρ_{out} , based on the obtained Kohn-Sham orbitals.

- Checking convergence:

Compare the new density ρ_{out} with the initial density ρ_{in} . If the change in density or energy satisfies the convergence criterion, the solution is complete.

- Density mixing:

If convergence is not achieved, mix the input and output densities to create an updated density for the next iteration:

$$\rho_{in}^{i+1} = (1-\alpha)\rho_{in}^{i} + \rho_{out}^{i} \qquad \text{(I.33)}$$

Here, α is a mixing parameter that controls the convergence speed.

- Repeating the process:

Iterate the procedure until the convergence condition is met, indicating self-consistency between the density and the Kohn-Sham potential.

This iterative process ensures that the Kohn-Sham orbitals and the electron density are refined at each step, ultimately leading to an accurate solution of the Kohn-Sham equation.

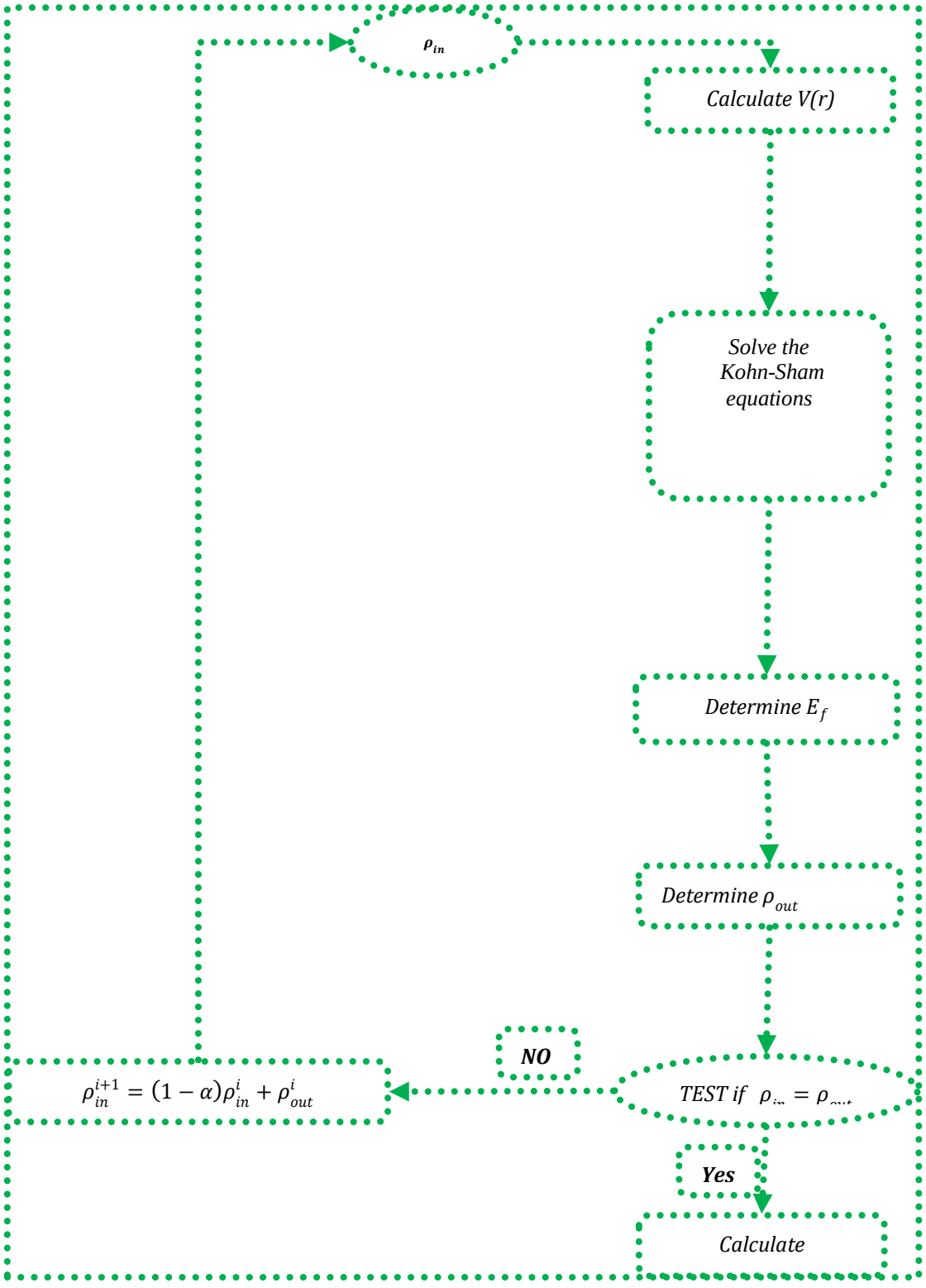

Figure (I. 1): Self-consistent calculation flowchart.

5- The Different Types of Approximation of $E_{xc}[\rho]$

Since there is no exact analytical expression for the exchange-correlation potential between electrons, various methods have been developed to approximate its values. The accuracy of the obtained results primarily depends on the mathematical formulation used for this potential [3].

5-1 Local Density Approximation (LSDA)

The Local Density Approximation (LSDA) was first introduced by Kohn and Sham in 1964 [22], where an inhomogeneous electronic system is approximated as a locally homogeneous electronic system by dividing the Brillouin zone into small regions. The exchange-correlation energy is then expressed by the following relation:

$$E_{XC}^{LSDA} = \int \rho(\vec{r})\, E_{xc}[\rho(\vec{r})] d\vec{r} \qquad \text{(I.34)}$$

$$V_{xc} = \frac{dE_{XC}^{LDA}[\rho]}{d\rho} = \varepsilon_{XC}^{LDA} + \rho(\vec{r})\frac{d\varepsilon_{XC}^{LDA}}{d\rho} \qquad \text{(I.35)}$$

For each spin up or down magnetic order, the total electron density becomes the sum of the two electron densities

$$\rho(\vec{r}) = \rho_{\uparrow}(\vec{r}) + \rho_{\downarrow}(\vec{r}) \qquad \text{(I.36)}$$

The Kohn-Sham equation for the two spins in the form [3]:

$$\begin{cases} \left(\frac{-\hbar^2}{2m}\nabla^2 + V_{eff}^{\uparrow}(\vec{r})\right)\varphi_i(\vec{r}) = \varepsilon_{KS}^{\uparrow}\varphi_i(\vec{r}) \\ \left(\frac{-\hbar^2}{2m}\nabla^2 + V_{eff}^{\downarrow}(\vec{r})\right)\varphi_i(\vec{r}) = \varepsilon_{KS}^{\downarrow}\varphi_i(\vec{r}) \end{cases} \qquad \text{(I.37)}$$

5-2 The Generalized Gradient Approximation (GGA)

The Generalized Gradient Approximation (GGA) is an advanced method developed to improve upon previous approximations by considering the non-homogeneity of the electron density. Unlike the Local Density Approximation (LDA), GGA accounts for variations in the electron density across different spatial regions. In this approach, the total energy of the electron system depends not only on the electron density ρ (r⃗)but also on its gradient ∇ρ (r⃗). This relationship is mathematically expressed as [23]:

$$E_{XC}^{GGA}[\rho(\vec{r})] = \int d^3\vec{r}\rho(\vec{r})\varepsilon_{XC}[\rho(\vec{r}), \nabla\rho(\vec{r})] \qquad (I.38)$$

5-3 The mBJ Approximation (modified Becke–Johnson) :

The modified Becke–Johnson (mBJ) potential is an improved exchange potential introduced by Tran and Blaha in 2009, aiming to provide more accurate calculations of the electronic band gap within the framework of Density Functional Theory (DFT).

While traditional approximations such as the Local Density Approximation (LDA) and the Generalized Gradient Approximation (GGA) are effective for predicting structural and mechanical properties, they notoriously underestimate the band gap of semiconductors and insulators. The mBJ approximation addresses this limitation by offering a more realistic description of the exchange potential that better reflects the true electronic behavior of materials.

Unlike LDA or GGA, the mBJ potential is not an energy functional but rather a semi-local exchange potential that depends on the local electronic density and its gradient, as well as the kinetic energy density. This allows the mBJ approximation to better reproduce the position of the conduction band and hence the band gap.

6- Full-Potential Linearized Augmented Plane-Wave Method (FP-LAPW)

The development of methods for solving the Kohn-Sham equations became essential for accurately determining the wave functions of electron systems. After extensive research, several approaches were introduced, including the OPW (Orthogonalized Plane Wave) method proposed by Herring in 1940 [24], the LMTO (Linear Muffin-Tin Orbital) method [25], and the FP-LAPW (Full-Potential Linearized Augmented Plane-Wave) method. The accuracy of these methods strongly depends on the quality of the effective potential employed.

6-1 The Augmented Plane Wave (APW) Method

The Augmented Plane Wave (APW) method, introduced by Slater [26], is based on the Muffin-Tin (MT) approximation [27] (see Figure I.2). In this approach, the crystal space is divided into two distinct regions:

- Muffin-Tin Spheres: Non-overlapping spheres of radius R_0 centered around atomic nuclei, where core electrons are localized.

- Interstitial Region: The space between these spheres, where free electrons move and interact with a nearly constant potential

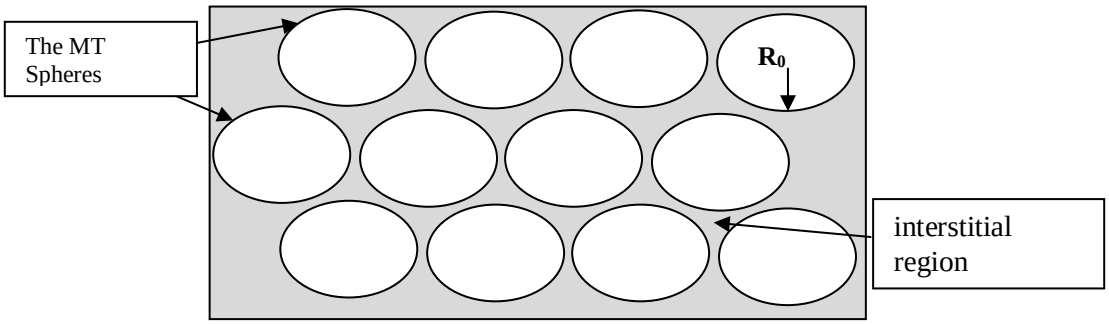

Figure (I. 2): Diagram of the distribution of the elementary cell in atomic spheres and in interstitial region.

Potential Distribution According to the MT approximation, the potential within the atomic spheres is assumed to be spherically symmetric, while in the interstitial region, it remains constant [3]. This can be expressed mathematically as :

$$V(\vec{r}) = \begin{cases} V(r) & r \leq R_0 \\ 0 & r > R_0 \end{cases} \qquad (I.39)$$

Wave Function Representation

Since the electronic environment differs between the two regions, the wave functions that describe electron behavior are also distinct.

- Inside the Muffin-Tin Spheres: The wave function is expressed as a sum of radial functions multiplied by spherical harmonics.
- In the Interstitial Region: The wave function is represented using plane waves.

The total wave function can be written as:

$$\varphi(\vec{r}) = \begin{cases} \sum_{l=0}^{\infty} \sum_{-m}^{m} A_{lm} U_l(r) Y_{lm}(r) & r \leq R_0 \\ \frac{1}{\sqrt{\Omega}} \sum_{G} C_G \, e^{i(\vec{K}+\vec{G})\vec{r}} & r > R_0 \end{cases} \qquad (I.40)$$

Where:

Ω is the unit cell volume.

$Y_{lm}$are the spherical harmonics.

A_{lm} are expansion coefficients.

U_l is the regular solution of the Schrödinger equation, given by [28]:

$$\left(-\frac{d^2}{dr^2}+\frac{l(l+1)}{r^2}V(\vec{r})\right)\mathrm{r}U_l = E_l U_l \qquad (\mathrm{I}.41)$$

where E_l is an energy parameter.

6-2 The Linearized Augmented Plane Wave Method (FP-LAPW)

One of the main drawbacks of the APW method is its computational inefficiency, primarily due to the dependence on the common radial function $U_l(r)$. Additionally, determining the radial function for each energy value E_l is challenging.

To overcome these limitations, Anderson [29] introduced an improvement to the APW method [30] by employing a Taylor series expansion to express the radial functions $U_l(r)$ in the following form:

$$U_l(r,E) = U_l(r,E_l) + (E_l - E)\frac{dU_l(r,E)}{dE}\Big|_{E=E_l} + \mathcal{O}(E_l - E)^2 \qquad (\mathrm{I}.42)$$

Where the term $\mathcal{O}(E-E_l)^2$represents the quadratic error.
After several simplifications, he has got the expression of potential inside and outside of Muffin-Tin balls as follows:

$$V(r) = \begin{cases} \sum_{lm}^{m} V_{lm}(r)Y_{lm} & r \le R_0 \\ \sum_{lm}^{m} V_k(r)e^{ikr} & r > R_0 \end{cases} \qquad (\mathrm{I}.43)$$

As well as the wave functions inside the spheres in terms of radial functions and their derivatives. Where the wave functions are written as follows [31,32]:

$$\Phi_{\vec{K}+\vec{G}}(\vec{r}) = \begin{cases} \sum_{lm}\left(A_{lm}U_l(r) + B_{lm}\dot{U}_l(r)\right)Y_{lm}(r) & r \le R_0 \\ \frac{1}{\sqrt{\Omega}}\sum_{G} C_G\, e^{i(\vec{K}+\vec{G})\vec{r}} & r > R_0 \end{cases} \qquad (\mathrm{I}.44)$$

Where :

$\vec{K}$: represents the wave vector.

$\vec{G}$: is the vector of the reciprocal lattice.

A_{lm}:: are coefficients corresponding to the function U_l.

B_{lm}: are coefficients corresponding to the function U_l.

We can determine the coefficients A_{lm} and B_{lm}, for each wave vector, and for each atom by applying the conditions of continuity of the basic functions in the vicinity of the limit of the spheres. After some simplifications we find the coefficient formula A_{lm} and B_{lm} in the following forms:

$$A_{lm} = \frac{4\pi {r_0}^2 i^L}{\sqrt{\Omega}} {Y^*}_{lm}(K+G) a_l(K+G) \qquad (\text{I}.45)$$

$$B_{lm} = \frac{4\pi {r_0}^2 i^L}{\sqrt{\Omega}} {Y^*}_{lm}(K+G) b_l(K+G) \qquad (\text{I}.46)$$

7. WIEN2K Software

WIEN2K is a comprehensive computational package composed of multiple Fortran-based subprograms. These subprograms serve as algorithms that numerically solve the equations governing crystalline systems within the framework of density functional theory (DFT). The software employs the full-potential linearized augmented plane wave (FP-LAPW) method, one of the most accurate techniques for calculating electronic and structural properties of materials [10].

The key subprograms within WIEN2K [33] and their specific roles are outlined in Figure I.3 and described as follows [10]:

- NN: Determines the distances between nearest-neighbor atoms up to a predefined limit, aiding in the calculation of the atomic sphere radius.
- SGROUP: Identifies the space group of the given compound.
- SYMMETRY: Computes the symmetry number and defines symmetry operations corresponding to the space group of the material.
- LSTART: Calculates electron densities for free atoms and determines the treatment of different orbitals in band structure calculations.

- KGEN: Generates a K-point mesh in the irreducible Brillouin zone (BZ), specifying the total number of K-points in the first BZ.
- DSTART: Constructs an initial electron density for the self-consistent field (SCF) cycle by superimposing atomic densities obtained from the LSTART step.

Following these preparatory steps, the program enters a self-consistency loop (SCF cycle), involving the following five key calculations:

- ✓ LAPW0 (POTENTIAL): Computes the Coulomb and exchange-correlation potentials (Hartree-Fock potential) using the total electron density. Additionally, it partitions space into muffin-tin (MT) spheres and the interstitial region.
- ✓ LAPW1 (BANDS): Solves the Kohn-Sham equation to determine eigenvalues and wave functions for valence electrons.
- ✓ LAPW2 (RHO): Derives the valence electron density based on the results from LAPW1.
- ✓ LCORE: Computes core electron eigenvalues and wave functions to determine core electron densities.
- ✓ MIXER: Combines the obtained electron densities to generate an updated self-consistent density for the next iteration.

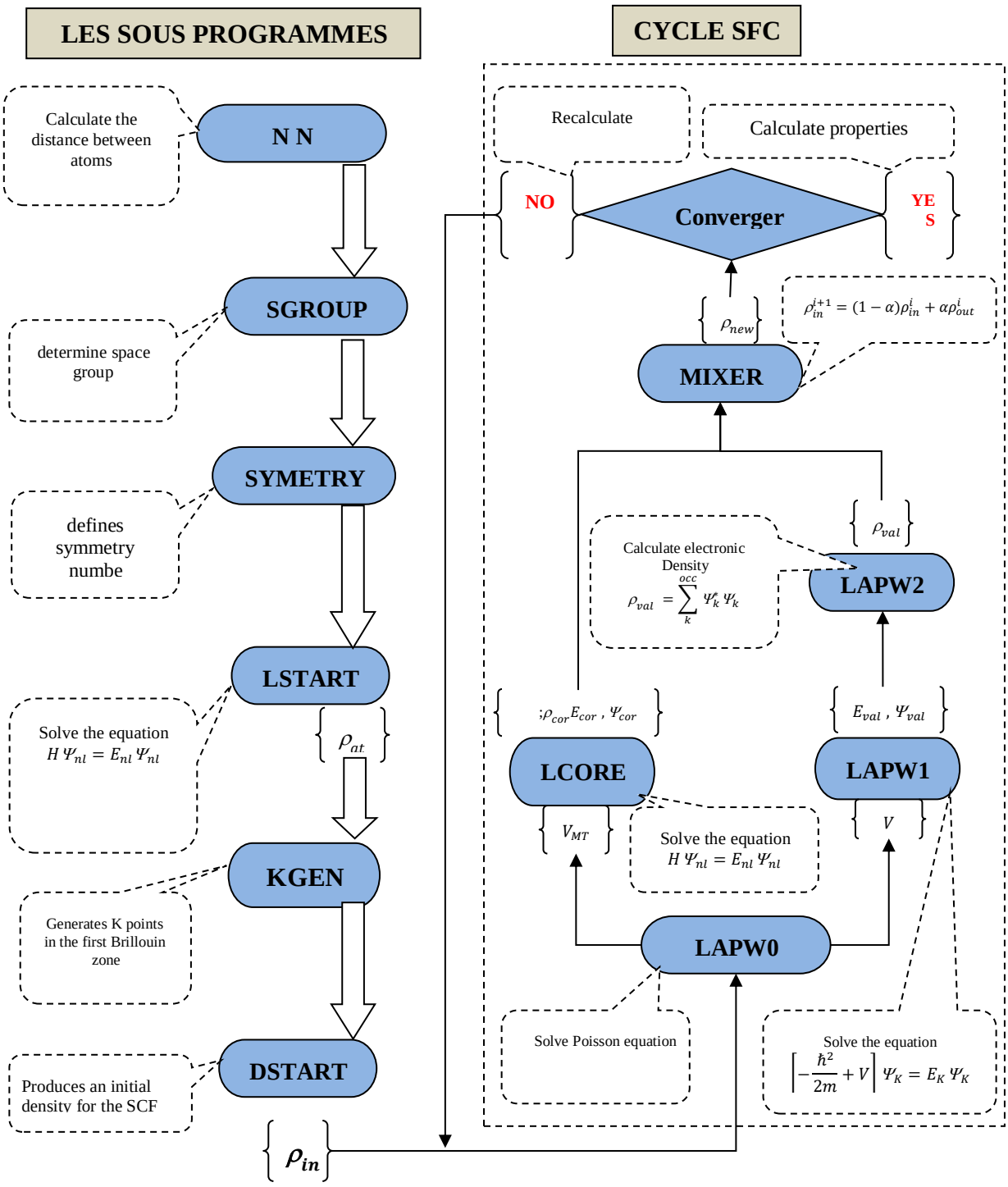

Figure (I.3): The flowchart of the Wien2k code subroutines[3].

8- References

[1] E SCHROEDINGER *Ann. Phys.* (1926).

[2] S S Essaoud, M Imadalou, and D E Medjadi *Int J Mod. Theo Phys.* **5** 8 (2016).

[3] S Saad Essaoud (2013).

[4] M Born and R Oppenheimer *Ann. Phys.* **389** 457 (1927).

[5] D R Hartree *Сборник Статей К Мультимедийному Электронному Учебно-Методическому Комплексу По Дисциплине «физика Атома И Атомных Явлений»отв Ред Шундалов МБ БГУ Физический Факультет* (1928).

[6] D R Hartree *The wave mechanics of an atom with a non-coulomb central field. Part II. Some results and discussion* (Cambridge University Press) p 111 (1928).

[7] D R Hartree *The wave mechanics of an atom with a non-coulomb central field. part iii. term values and intensities in series in optical spectra* (Cambridge University Press) p 426 (1928).

[8] G Shadmon and I Kelson *Nucl. Phys. A* **241** 407 (1975).

[9] J F Berger (1991).

[10] S Saad Essaoud *DOCTORAT THESIS* (2020).

[11] L H Thomas *Math. Proc. Camb. Philos. Soc.* **23** 542 (1927).

[12] E Fermi *Z. Für Phys.* **48** 73 (1928).

[13] ل مروة *Master Thesis* (UNIVERSITE MOHAMED BOUDIAF-M'SILA) (2021).

[14] آ قريشي *Master Thesis* (UNIVERSITE MOHAMED BOUDIAF-M'SILA) (2021).

[15] R M Dreizler and E K U Gross (1990).

[16] R.M. Dreizler, Providência (1985).

[17] R Stowasser and R Hoffmann *J. Am. Chem. Soc.* **121** 3414 (1999).

[18] A Seidl, A Görling, P Vogl, J A Majewski, and M Levy *Phys. Rev. B* **53** 3764 (1996).

[19] C Fiolhais, F Nogueira, and M A Marques *A primer in density functional theory* (Springer Science & Business Media) (2003).

[20] F M Bickelhaupt and E J Baerends *Rev. Comput. Chem.* **15** 1 (2000).

[21] J A Pople, P M Gill, and B G Johnson *Chem. Phys. Lett.* **199** 557 (1992).

[22] W Kohn and L J Sham *Phys. Rev.* **140** A1133 (1965).

[23] D M Ceperley and B J Alder *Phys. Rev. Lett.* **45** 566 (1980).

[24] C Herring *Phys. Rev.* **57** 1169 (1940).

[25] H L Skriver *The LMTO Method: Muffin-Tin Orbitals and Electronic Structure* (Berlin Heidelberg : Springer-Verlag) (1984).

[26] J C Slater *Phys. Rev.* **51** 840 (1937).

[27] O K Andersen and T Saha-Dasgupta *Phys. Rev. B* **62** R16219 (2000).

[28] O K Andersen *Phys. Rev. B* **12** 3060 (1975).

[29] M Petersen, F Wagner, L Hufnagel, M Scheffler, P Blaha, and K Schwarz *Comput. Phys. Commun.* **126** 294 (2000).

[30] D R Hamann *Phys. Rev. Lett.* **42** 662 (1979).

[31] M Weinert *J. Math. Phys.* **22** 2433 (1981).

[32] P. Blaha, K. Schwarz, G. Madsen, D. Kvasnicka, J. Luitz (2001).

CHAPTER 2:

RESULTS AND DISCUSSION

1)Introduction 29
2) Calculation Details 29
3) Results and discussions 30
3-1) Structural properties 30
3-2) Electronic Properties: 34
3-2-1) Energy Bands: 34
3-2-2) Total Density of States (TDOS) Partial Density of States (PDOS): 36
4)Thermodynamic Properties 39
4-1) Heat Capacity Cv 40
4-2) Entropy S: 42
4-3) Thermal Expansion Coefficient α: 43
4.5 The Debye temperature θ_D : 45
5)The elastic Properties : 47
References 50

1) Introduction

Using a theoretical framework, the study examined the structural, elastic, electrical, and thermodynamic characteristics of the MAX phase compounds V2SnC and V2SnN. Lattice constants and bulk modulus were used to evaluate the structural stability. Fundamental elastic constants and derived parameters were used to assess the elastic characteristics. Band structure and density of states computations were used to investigate the electronic behavior. In order to evaluate their possible performance in high-temperature and high-pressure settings, the thermodynamic properties—such as heat capacity, entropy, thermal expansion coefficient, Debye temperature, and bulk modulus—were investigated under various temperature and pressure cases.

2) Calculation Details

Structural, elastic and electronic properties have been estimated using the full-potential linearized augmented plane wave method (FP-LAPW) implemented in the WIEN2k program [1]. The structural properties have been calculated with both generalized gradient approximation (GGA) [2] to achieve the exchange-correlation potential. Whereas modified Becke-Johnson potential (mBJ) [3] has been used to improve the electronic behavior of all the studied compounds. To study the core and valence electrons separately; the Muffin-Tin approximation is applied where the core electrons are modelled by spherical harmonic functions with angular momentum up to l_{max} = 10 and Gaussian factor G_{max} equal to 12, whereas the valence electrons are depicted by plane wave functions, which are located outside the atomic spheres (interstitial region). The cutoffs of $R_{MT}*K_{max}$ used in our calculation are equal to 8 for all compounds, where K_{max} is the largest reciprocal lattice vector used in the plane wave expansion and R_{MT} represents the smallest MT sphere radii. For Brillouin zone (BZ) integration; a mesh of (17×17×3) special k-points were used for all MAX phase compounds in the irreducible wedge to minimize the total energy for all compounds. The criteria of convergence in the self-consistent were achieved when the difference in energy between two consecutive cycles is less than 10^{-4} Ry. The optimized atomic positions are obtained for minimization of the internal forces to vales less than 10^{-3} Ry/a.u. GIBBS2 [4,5] code was employed to obtain the thermal which is based on semi-classical Boltzmann theory and the quasi-harmonic Debye model.

3) Results and discussions

3-1) Structural properties

Both compounds V_2SnN and V_2SnC exhibit a hexagonal crystalline architecture characterized by the space group (194) P63/mmc. As illustrated in Figure (II-1), the unit cell of these materials comprises eight atoms, with the atomic positions delineated in fractional coordinates presented in TABLE (II-1).

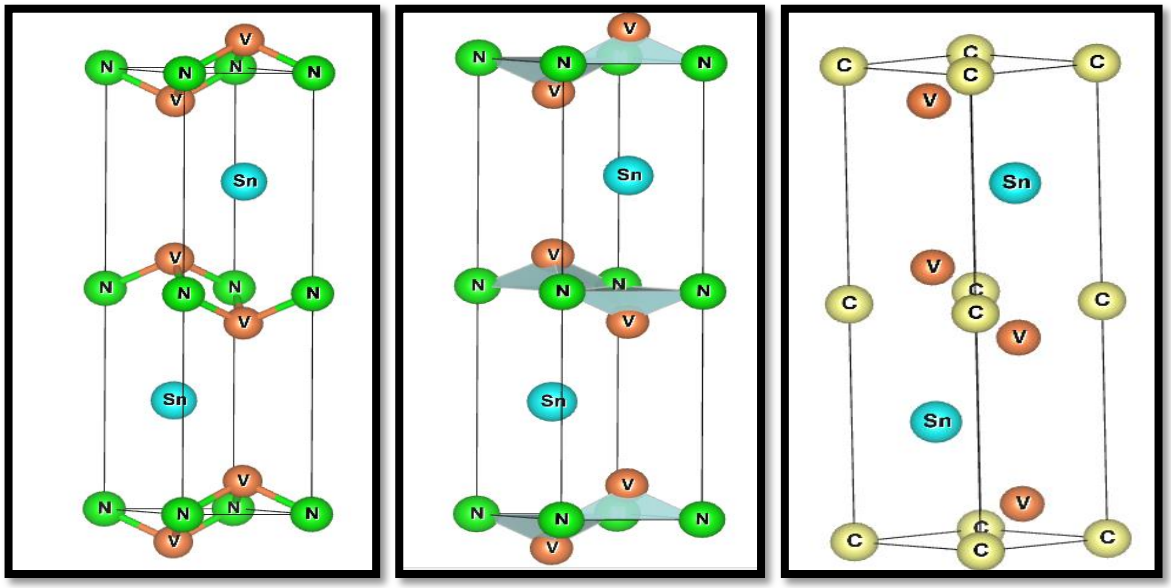

FIGURE(II-1): Crystal structure of V_2SnC and V_2SnN compounds

V_2SnC		V_2SnN	
Atome	Position	Atome	Position
Sn	(0.66667;0.33333;0.25000)	Sn	(0.66667;0.33333;0.25000)
Sn	(0.33333;0.66667;0.75000)	Sn	(0.33333;0.66667;0.75000)
C	(0.00000;0.00000;0.00000)	N	(0.00000;0.00000;0.00000)
C	(0.00000;0.00000;0.50000)	N	(0.00000;0.00000;0.50000)
V	(0.33333;0.66667;0.07506)	V	(0.33333;0.66667;0.07087)
V	(0.66667;0.33333;0.92494)	V	(0.66667;0.33333;0.92913)
V	(0.66667;0.33333;0.57506)	V	(0.66667;0.33333;0.57087)
V	(0.33333;0.66667;0.42494)	V	(0.33333;0.66667;0.42913)

TABLE(II-1) : Atomic positions for V_2SnC and V_2SnN compounds

To find the equilibrium structural properties of V_2SnC and V_2SnN, we performed GGA approximation calculations to determine how the total energy of their unit cells changed with varying volumes. The resulting energy-volume data was then plotted and fitted using the Murnaghan equation[6]

$$E(V) = E_0 + \frac{B}{B'(B'-1)}\left[V\left(\frac{V_0}{V}\right)^{B'} - V_0\right] + \frac{B}{B'}(V - V_0) \qquad (II\text{-}1)$$

Where the parameters represent:

- V_0 : The volume of the cell at equilibrium.

- E_0: The total energy of the primitive cell at equilibrium.

- B: Bulk modulus.

- B': Pressure derivative of the bulk modulus.

The expression for the bulk modulus is given by the equation:

$$B = -V\frac{\partial P}{\partial V} = V\frac{\partial^2 E}{\partial V^2} \qquad (II\text{-}2)$$

Using the data presented in FIGURE (II-2) and FIGURE (II-3), we first identified the minimum energy volumes for V_2SnN and V_2SnC. From these, we proceeded to calculate their respective lattice constants 'a' (Å) and bulk moduli, as detailed in TABLE (II-2).

A key observation is that V_2SnC possesses a higher bulk modulus compared to V_2SnN. Given that the bulk modulus quantifies a material's resistance to deformation under pressure, this implies V_2SnC is more mechanically robust. This difference serves as a valuable indicator of the high mechanical stability of both V_2SnC and V_2SnN under pressure. Additionally, our analysis of the volume change as a function of pressure reveals a nearly linear decrease in crystal volume with increasing pressure, providing clear evidence of no structural collapse within the tested pressure range.

V_2SnN		V_2SnC	
$V_0(a.u)^3$	710.7055	$V_0(a.u)^3$	716.5291
B(GPa)	200.0260	B(GPa)	195.2101
B'(GPa)	5.5966	B'(GPa)	5.0806
$E_0(Ry)$	-32510.675985	$E_0(Ry)$	-32444.064094
$a(A^0)$	3.084	$a(A^0)$	3.092
$c(A^0)$	12.773	$C(A^0)$	12.808

TABLE(II-2) : Values of the structural parameters obained for V_2SnC and V_2SnN compounds and calculated by GGA approximation

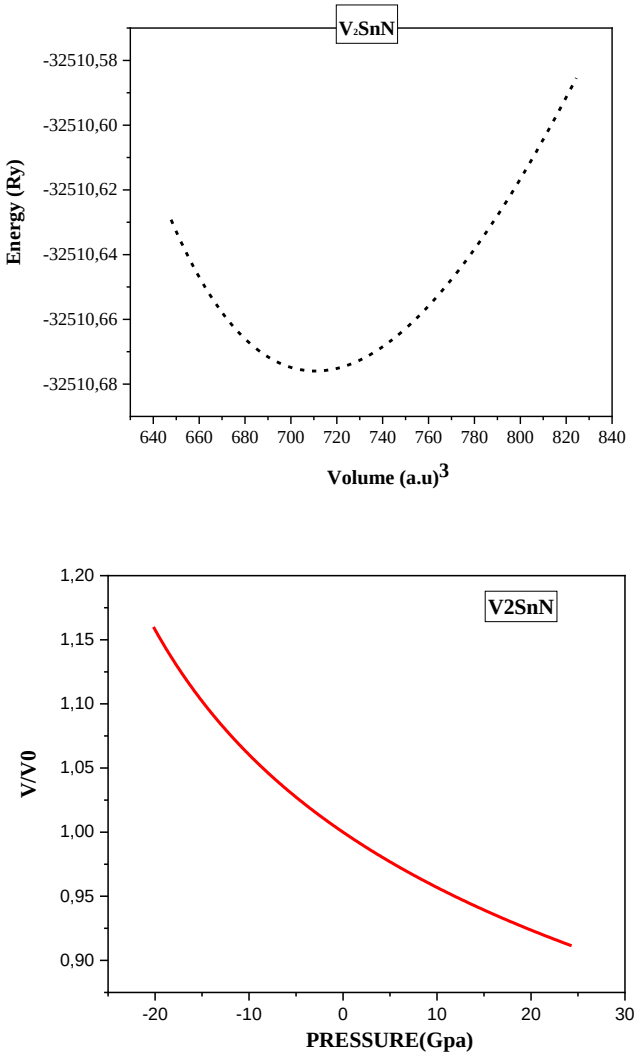

FIGURE(II-2) : Total Energy-Volume and volume-pressure Curvesof V_2SnN calculated using GGA-sol approximations.

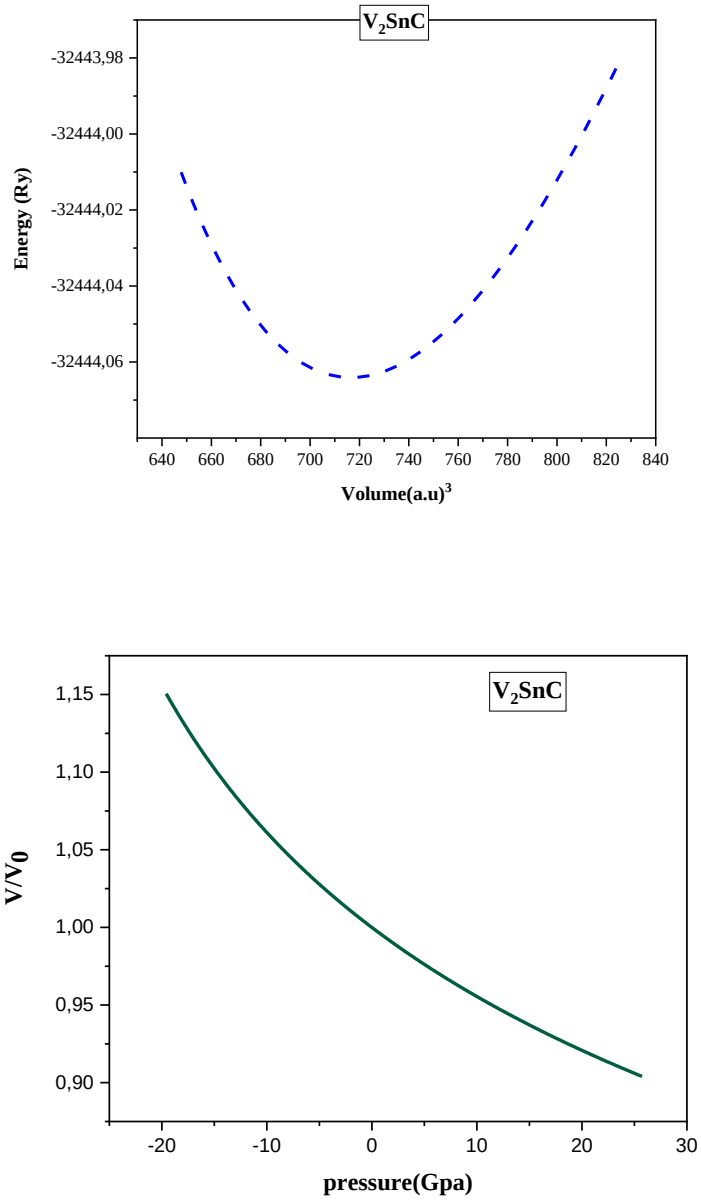

FIGURE (II-3): Total Energy-Volume and volume-pressure Curves of V_2SnN calculated using GGA-sol approximations

. 3-2) Electronic Properties:

Studying the electronic properties is essential for identifying the potential electronic or electrical applications of materials. In this work, we investigated the electronic band structure to determine whether the studied compounds exhibit insulating, metallic, or semiconducting behavior. Additionally, we analyzed the density of states to identify the atomic orbitals contributing to each band, thereby deepening our understanding of the bonding characteristics within the material.

3-2-1) Energy Bands:

The energy bands for both compounds, V_2SnC and V_2SnN, were studied in their stable hexagonal structure within the first Brillouin zone. High-symmetry points were traced along the path (Γ→ M→ K → Γ →A). Through analyzing the energy band diagrams, which were calculated using mBJ approximations. As evident from FIGURE (II-5), which presents the band structure spectra of V_2SnC and V_2SnN, we observed a significant overlap between the valence and conduction bands. This finding unequivocally indicates the metallic nature of both compounds.

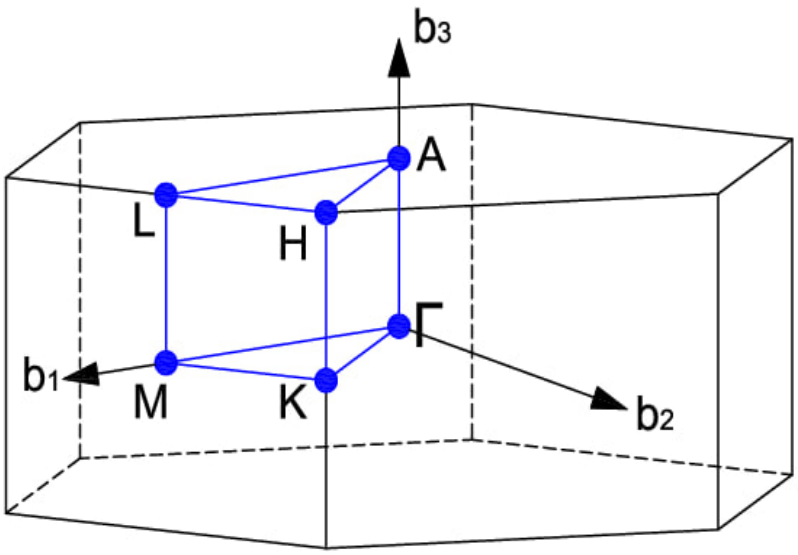

FIGURE (II-4): The hexagonal Brillouin zone

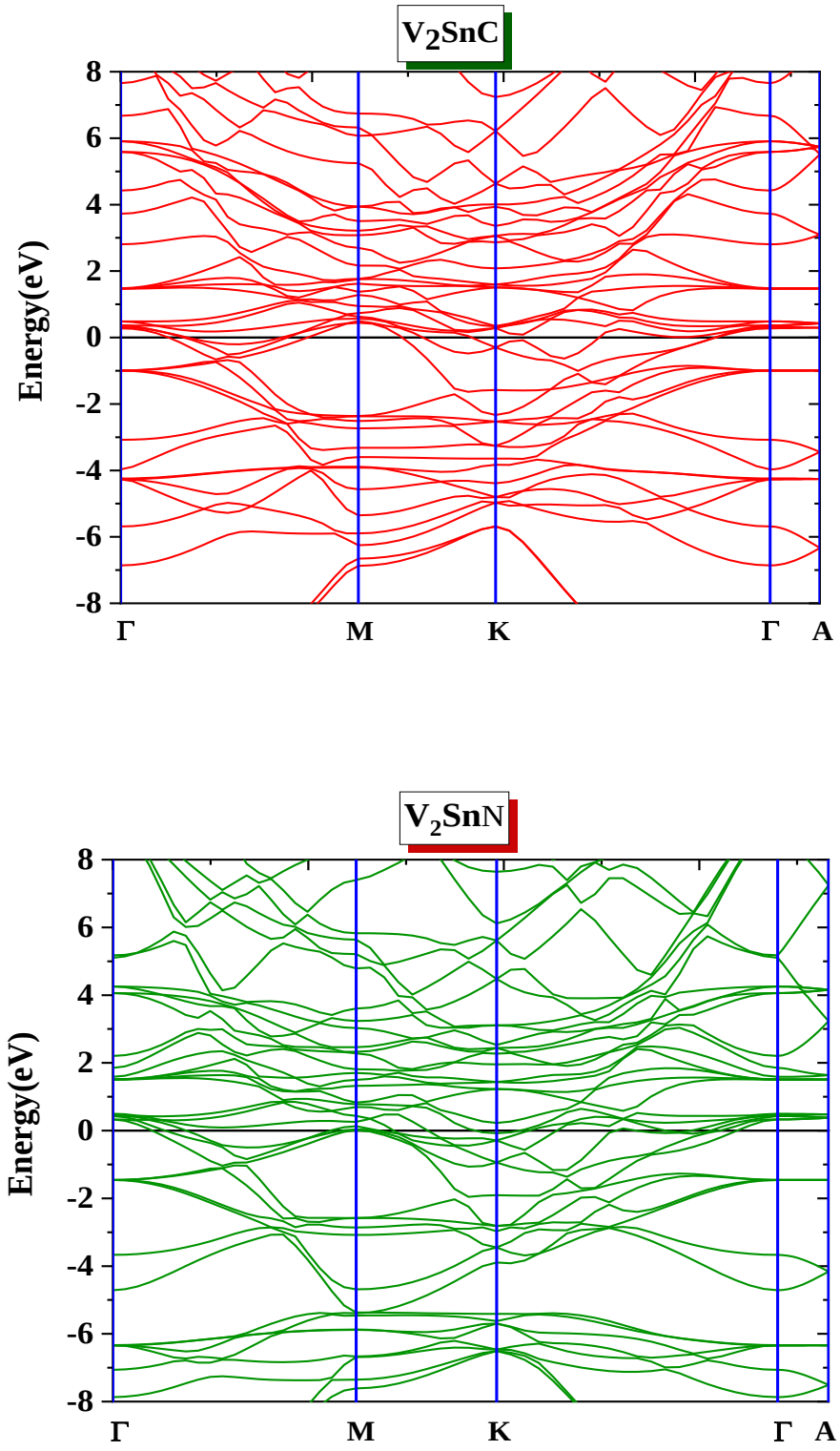

FIGURE (II-5): band structure spectra for both compounds V_2SnC and V_2SnN

3-2-2) Total Density of States (TDOS) Partial Density of States (PDOS):

To identify the atomic orbits contributing to the formation of both conduction and valence bands, the total and partial density of states (DOS) using mBJ method for for both compounds.

The distribution curves of atomic orbital contributions to the formation of valence and conduction bands are organized as follows:

1. The presence of electronic states at the Fermi level in both compounds confirms their metallic nature, as there is no energy gap separating the valence and conduction bands.
2. The density of states (DOS) profiles of V_2SnN and V_2SnC exhibit notable differences, highlighting the impact of substituting the nitrogen atom with carbon on the energy distribution and the involvement of different atomic orbitals.

The energy-resolved contributions of atomic orbitals, as illustrated in FIGURE (II-6) for V_2SnN and FIGURE (II-7) for V_2SnC, can be categorized into the following regions:

➤ For V_2SnN FIGURE (II-6):

- **[-7 eV to -5 eV]:** Predominantly derived from the *s*-orbital electrons of the Sn atom.
- **[-5 eV to 5 eV]:** Major contributions from the *d* and *p* orbitals of V, as well as the *p* orbitals of N.

➤ For V_2SnC FIGURE (II-7):

- **[-8 eV to -5 eV]:** Dominated by the *s* orbitals of Sn, with minor contributions from the *s* orbitals of C.
- **[-5 eV to 5 eV]:** Strong contributions from the *p* orbitals of both C and Sn, along with significant *d*-orbital contributions from V.

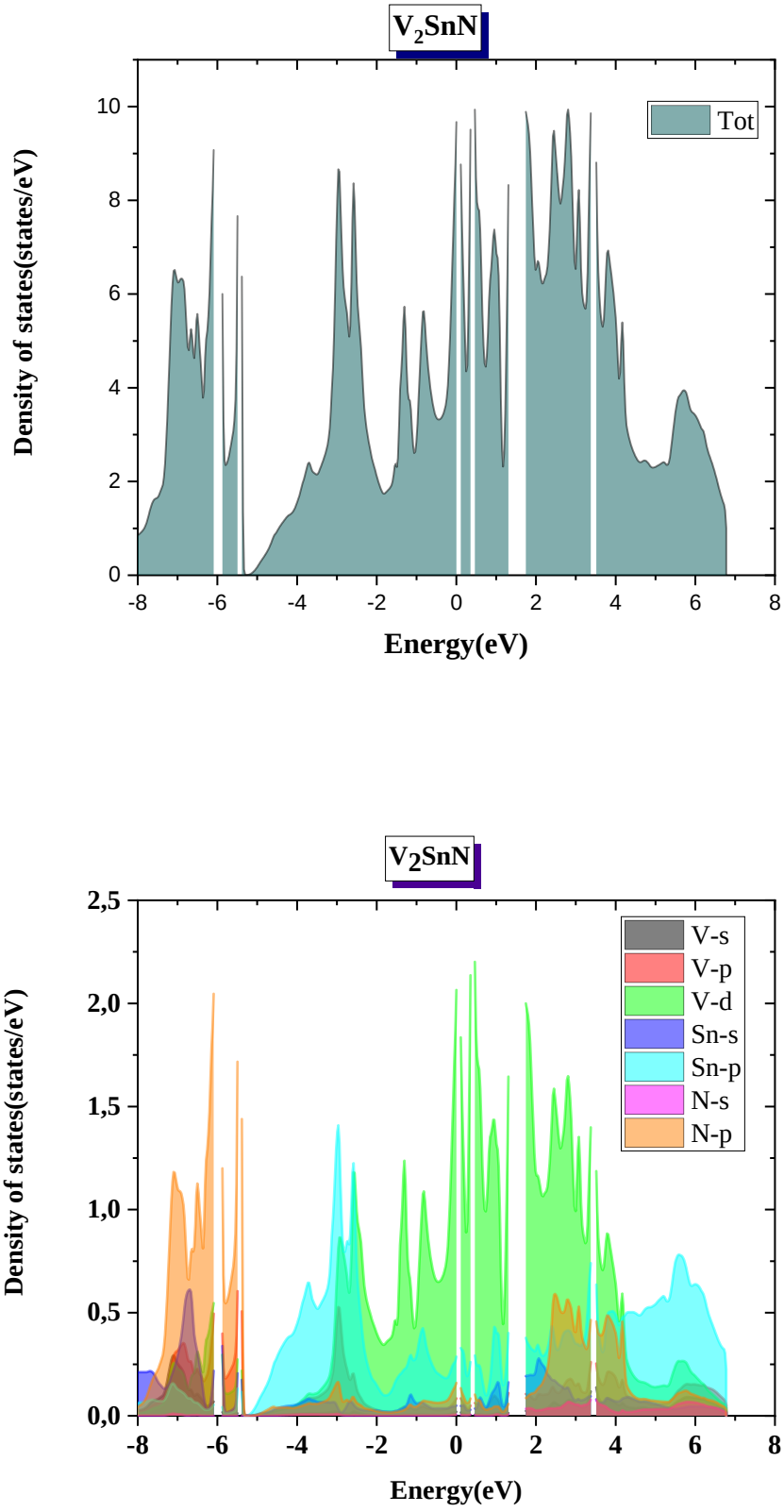

FIGURE(II-6): Total and partial density of states of V_2SnN

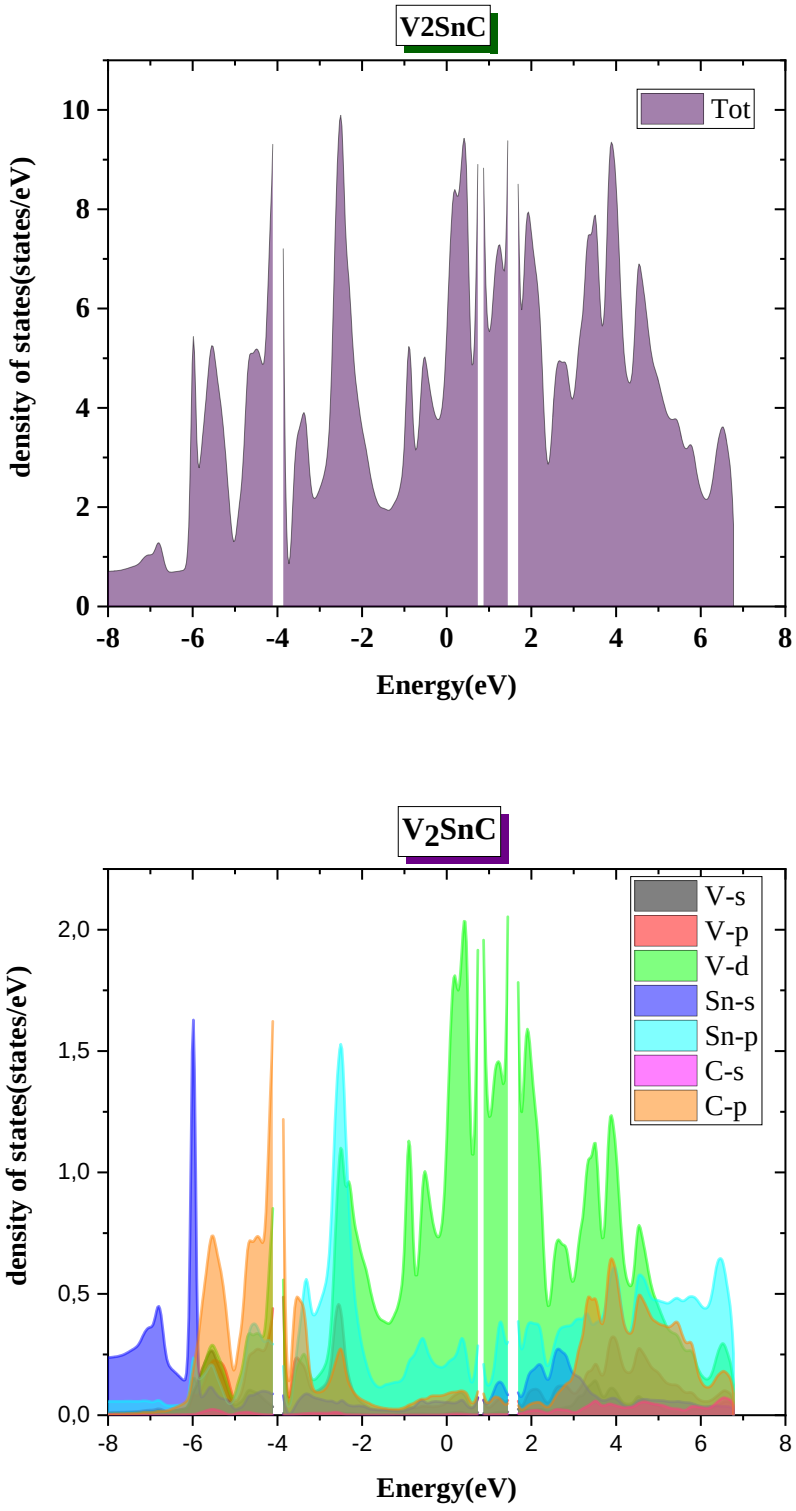

FIGURE(II-7): Total and partial density of states of V_2SnC

4) Thermodynamic Properties

First-principles calculations were performed using the WIEN2k package at zero Kelvin, where atomic vibrational effects were neglected in the Hamiltonian by applying the Born–Oppenheimer approximation. To investigate the temperature-dependent thermodynamic behavior, we employed the quasi-harmonic approximation (QHA) as implemented in the GIBBS2 code [4,5]. The thermodynamic stability of a solid under given pressure and temperature conditions is governed by the Gibbs free energy, which is defined as:

$$G^*(x, V; P, T) = E_{sta}(x, V) + PV + A^*_{vib}(x, V; T) + F^*_{el}(x, V; T) \quad (II-3)$$

Here, E_{sta} represents the total static energy, PV accounts for hydrostatic pressure, and A^*_{vib} and F^*_{el} correspond to the non-equilibrium vibrational and electronic free energy terms, respectively. The vibrational energy contribution A^*_{vib} is evaluated based on the Debye model, using the phonon density of states g(ω):

$$A^*_{vib} = \int_0^{\infty} \left[\frac{\omega}{2} + k_B T \, Ln\,(1 - e^{-\frac{\omega}{k_B T}})\right] g(\omega) d\omega \quad (II-4)$$

$$F^*(x, V; T) = E_{sta}(x, V) + A^*_{vib}(x, V; T) \quad (II-5)$$

in this equation, n is the number of atoms per unit volume, D (θ / T) represents the Debye integral, which is given by:

$$D(x) = \frac{3}{x^3} \int_0^x \frac{y^3 e^{-y}}{1 - e^{-y}} \, dy \quad (II-6)$$

The equilibrium state (for pressure (P) and a temperature (T) given) is obtained by the minimization of:

$$\left(\frac{\partial G^*(V, P, T)}{\partial V}\right)_{P,T} = 0 \quad (II-7)$$

Once equilibrium is established, other thermodynamic quantities such as entropy S, heat capacity at constant volume C_v , and thermal expansion coefficient α can be derived as follows:

$$S = -3nk_B \ln\left(1 - e^{-\Theta_D/T}\right) + 4nk_B D(\Theta_D/T) \quad (II-8)$$

$$C_v = 12nk_B D(\Theta_D/T) - \frac{9nk_B \Theta_D/T}{e^{\Theta_D/T} - 1} \quad (II-9)$$

$$\alpha = -\frac{1}{V}\left(\frac{\partial V}{\partial T}\right)_P = \frac{\gamma C_v}{V B_T} \quad (II-10)$$

In this section, we investigate the thermodynamic properties of the compounds V_2SnC and V_2SnN under the influence of pressure and temperature. The properties studied include the heat capacity at constant volume (Cv), entropy (S), thermal expansion coefficient (α), bulk modulus (B), Debye temperature (θD), and volume ($u.a^3$). The pressure range considered is from 0 to 40 GPa, while the temperature range extends from 0 K to 1200 K.

4-1) Heat Capacity Cv

Heat capacity reflects a material's ability to absorb thermal energy, generally increasing with the number of atomic vibrational degrees of freedom. On a microscopic level, entropy quantifies disorder within a system, corresponding to the number of accessible microstates. As temperature rises, atoms vibrate more vigorously, enabling new vibrational configurations to emerge [7].

Figures (II.8) and (II.9) for V_2SnC and V_2SnN compounds illustrate that the constant-volume heat capacity (Cv) follows the Dulong–Petit law [8] above 700 K, plateauing at approximately 100 J/mol·K. At low temperatures (below 200 K), Cv increases proportionally to T3. Additionally, we observed that Cv decreases as pressure increases (from 0 to 40 GPa).

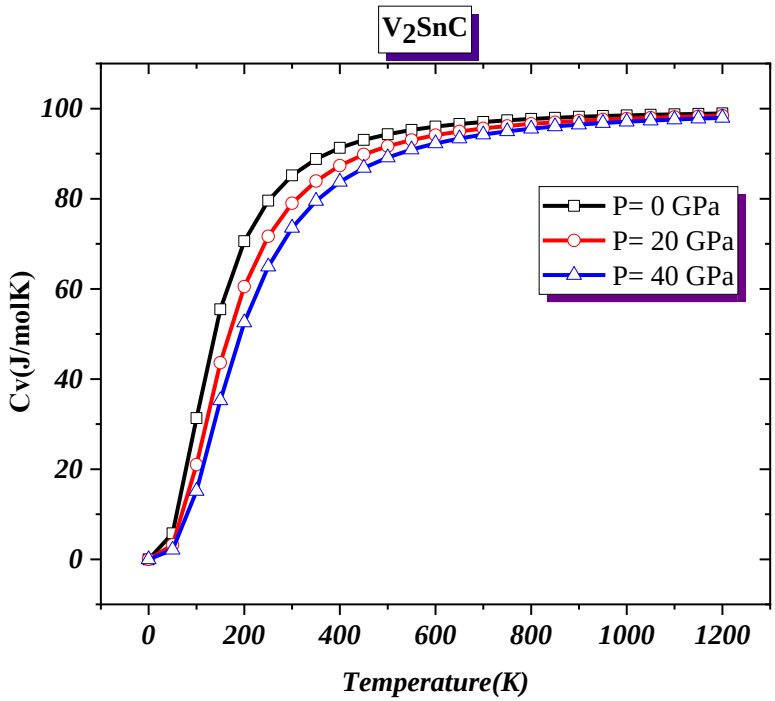

FIGURE (II-8): variation of the heat capacity "Cv" of the compound V_2SnC as a function of temperature

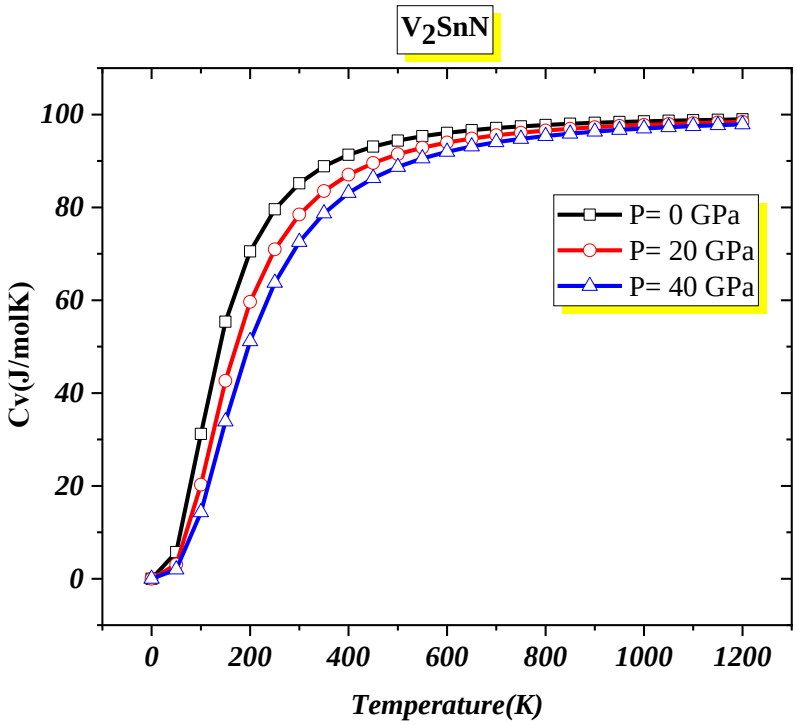

FIGURE(II-9) : variation of the heat capacity "Cv" of the compound V_2SnN as a function of temperature

4-2) Entropy S :

Entropy is a multifaceted concept, utilized across various disciplines and viewpoints. From a thermodynamic perspective, it can be defined at two levels: microscopically, entropy serves as a measure of a system's disorder (chaos and randomness), representing the number of possible states the system can occupy. This is expressed as S=k Ln Ω, where Ω represents the number of possibilities or arrangements that a compound can occupy, while k represents the Boltzmann constant. On the macroscopic level, entropy is the amount of internal energy of a substance that cannot be converted into useful work and can be considered as unusable energy for obtaining work[4,5].

According to the obtained results, the entropy of both compounds increases almost linearly with increasing temperature, while it decreases with increasing pressure.

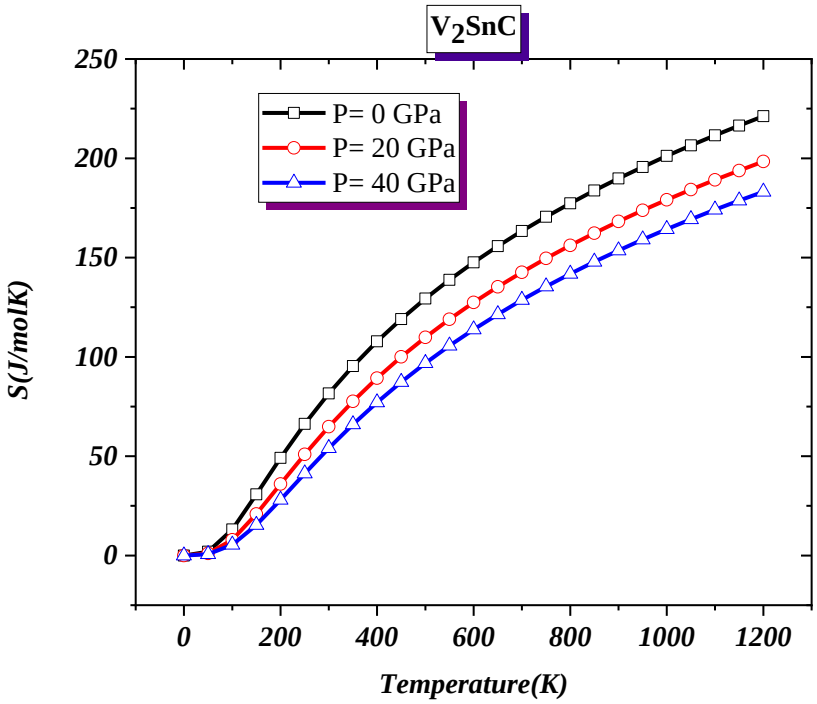

FIGURE(II-10): variation of the entropy (S) as function of temperature of V_2SnC

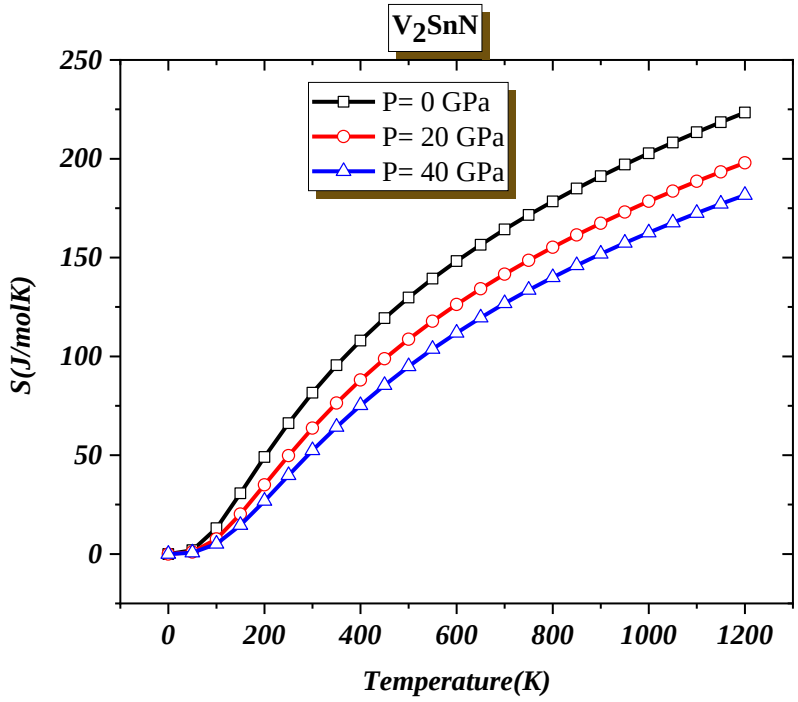

FIGURE (II-11): variation of the entropy (S) as function of temperature of V_2SnN

4-3) Thermal Expansion Coefficient α:

The thermal behavior of solid-state materials plays a crucial role in the design and reliability of electronic devices, especially those that generate significant heat during operation. One of the most critical thermal properties of these materials is the thermal expansion coefficient. This property is important because excessive expansion can cause mechanical failure, damage to device components, or induce stress that may negatively affect the electronic performance of the system [4,5].

From the curves below, it is observed that both compounds exhibit a moderate thermal expansion coefficient. This coefficient is influenced by both temperature and pressure, increasing with rising temperature and decreasing with increasing pressure

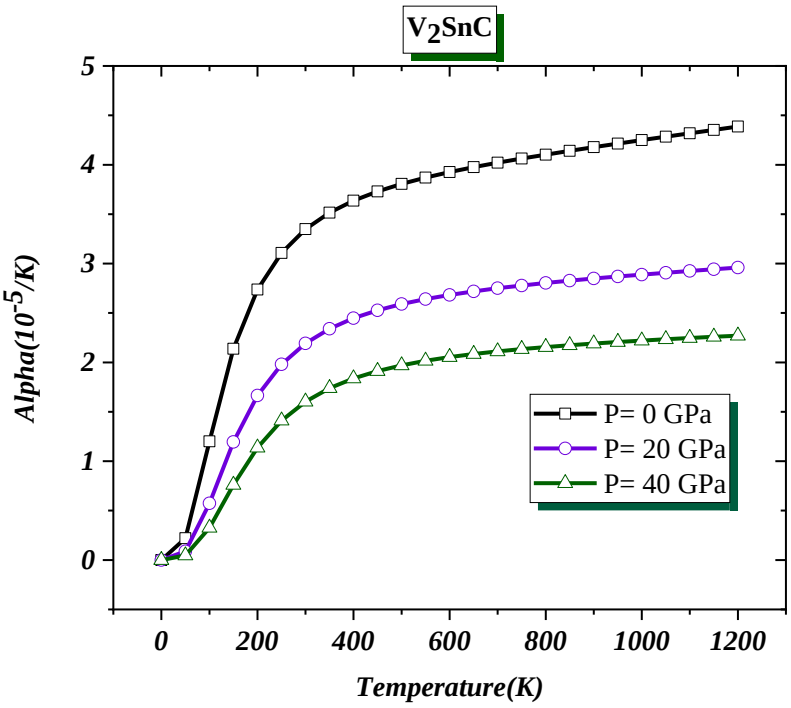

FIGURE (II-12): variation of the thermal expansion coefficient (α) as function of temperature of V_2SnC

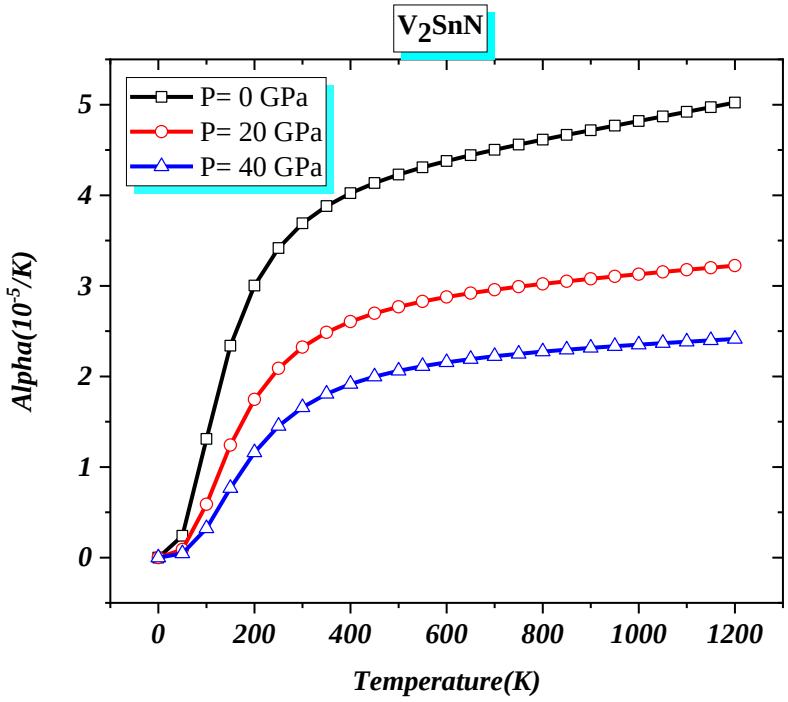

FIGURE (II-13): variation of the thermal expansion coefficient (α) as function of temperature of V_2SnN

4.5 The Debye temperature θ_D :

The Debye temperature, θD, is a characteristic temperature that reflects the highest normal-mode vibration (phonon) frequency in a crystalline solid. The data extracted from FIGURE (II-14), which illustrates the variation of the Debye temperature as a function of both pressure and temperature, show that the Debye temperature decreases linearly with increasing temperature at constant pressure, while it increases with rising pressure.

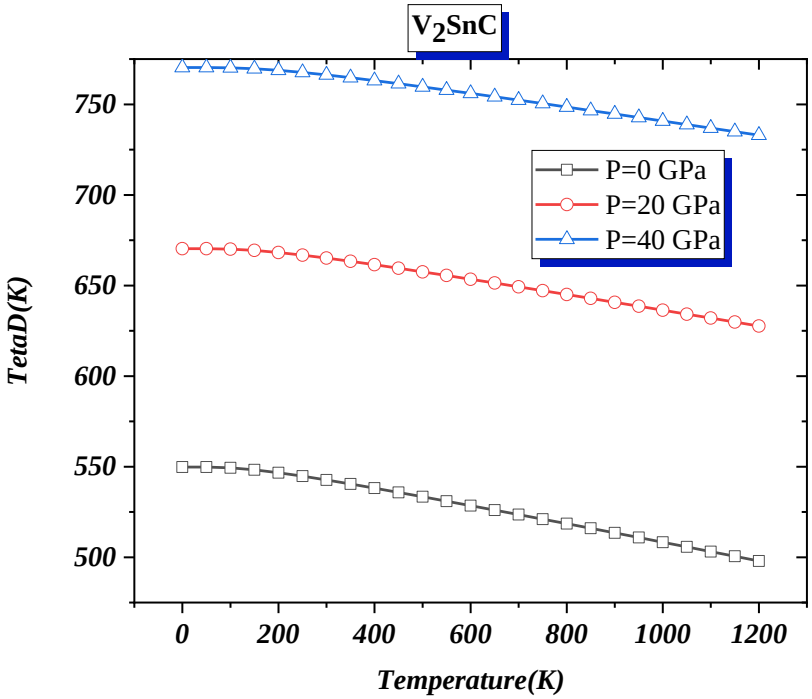

FIGURE (II-14): variation of The Debye temperature θD as function of temperature of V_2SnC

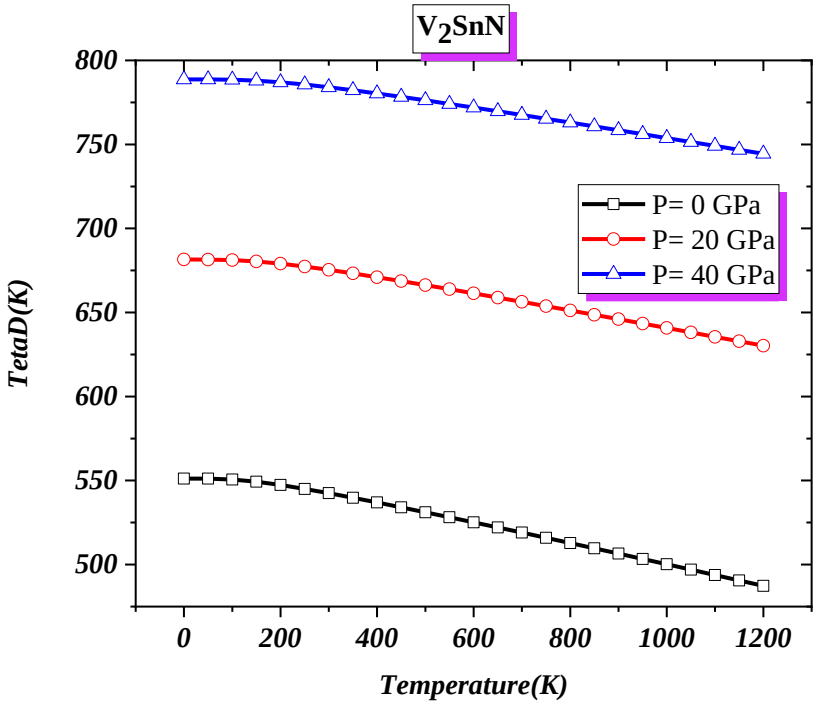

FIGURE (II-15): variation of The Debye temperature θD as function of temperature of V_2SnN

5) The elastic Properties :

The elastic constants C_{ij} for the V_2SnC and V_2SnN compounds were obtained using the second-order derivatives of the fitted polynomials of the total energy with respect to volume-conserving strains that break the symmetry of the hexagonal crystal structure. These constants allow us to explore the mechanical behavior of the materials and the influence of the constituent atoms V, Sn, and either C or N on the mechanical stability and elasticity.

The obtained results such as bulk (*B*),shear modulus (*G*), Young's modulus (*Y*), anisotropy (*A*), and Poisson's ratio (υ) are listed in Table 2, which calculated as a function of elastic constants C_{ij} using the following formulas [9,10]:

$$B = \frac{2}{9}\left(C_{11} + C_{12} + 2\,C_{13} + \frac{C_{33}}{2}\right) \quad (II-11)$$

$$G = \frac{1}{15}(2\,C_{11} + C_{33} - C_{12} - 2\,C_{13}) + \frac{1}{5}\left(2\,C_{44} + \frac{1}{2}(C_{11} - C_{12})\right) \quad (II-12)$$

$$Y = \frac{9\,B\,G}{3\,B + G} \quad (II-13)$$

$$\upsilon = \frac{3\,B - 2\,G}{2\,(3B + G)} \quad (II-14)$$

$$A = \frac{2\,C_{44}}{C_{11} - C_{12}} \quad (II-15)$$

$$f = \frac{C_{11} + C_{12} - 2\,C_{13}}{C_{33} - C_{13}} \quad (II-16)$$

The values of the elastic constants (Table 2) confirm that both V_2SnC and V_2SnN satisfy the Born-Huang mechanical stability criteria for hexagonal crystals:
$(C_{11} > |C_{12}|,\ C_{44} > 0$, and $(C_{11} + C_{12})C_{33} > 2C_{13}^2)$ [11].

The Bulk modulus (B) of the studied compounds; which expresses the response of these materials against any uniform compression they undergo; was calculated again depending on the elastic constants, shows comparable values for both V_2SnC (134.13 GPa) and V_2SnN (133.15 GPa), indicating similar volumetric incompressibility. In contrast, the shear modulus (G), indicative of resistance to shape change, is significantly

higher for V_2SnC (83.38 GPa) than V_2SnN (55.26 GPa), revealing a greater ability of V_2SnC to resist shear deformation.

Using the three values B, G, and C_{44}, we can estimate the brittleness/ductility and machinability of the studied materials by calculating the ductility factor $U_d = B/G$[38] and the machinability factor $U_M = B/C_{44}$[12]. The values obtained are 1.61 for V_2SnC and 2.41 for V_2SnN. According to the Pugh criterion, materials with B/G>1.75 are ductile, while those with lower values are brittle. Thus, V_2SnN exhibits ductile behavior, whereas V_2SnC lies on the borderline between brittleness and ductility , the machinability factor $U_M = B/C_{44}$ indicates better machinability for V_2SnN (2.32) compared to V_2SnC (1.43). The G/B ratio is often used to evaluate the dominant bonding nature: ionic compounds tend to have G/B ≈ 0.6, while covalent compounds approach 1.1 [13]. The calculated values (0.62 for V_2SnC and 0.42 for V_2SnN) imply that both compounds are dominantly ionic, with V_2SnN having a more pronounced ionic character.

Young's modulus (Y), which measures stiffness under uniaxial stress, is significantly higher for V_2SnC (207.21 GPa) than for V_2SnN (145.64 GPa), indicating that V_2SnC is stiffer.

The Poisson's ratio (υ) values (0.24 for V_2SnC and 0.32 for V_2SnN) suggest that V_2SnC is more covalent in nature, while V_2SnN tends toward metallic bonding characteristics [14,15].

The anisotropy factor (A) shows both materials are anisotropic, with A = 1.13 for V_2SnC and A = 1.14 for V_2SnN. Neither compound is isotropic, as their A values deviate from unity.

	V_2SnC	V_2SnN
C_{11}	227.993591	179.528599
C_{12}	61.202004	78.971341
C_{13}	97.572322	100.629289
C_{33}	250.543246	253.604417
C_{44}	93.887426	57.499368
B(GPa)	134.12982	133.152012
G(GPa)	83.383508	55.263718
G/B	0.62166271	0.4150423
Y	207.207422	145.635595
υ	0.24250	0.31764
A	1.12580529	1,14361447
U_d	1.608589	2.4093929
U_M	1.428623	2.315712

TABLE (II-3) : Elastic constants (C_{ij}), Young's modulus Y, Poisson's ration (υ), Anisotropy(A), Bulk (B) and Shear modulus (G), G/B ratio, *f*-index , ductility U_d and machinability U_M factors of M_2AX phases (M= V , A= Sn, X = C or N)

References

[1] P. Blaha, K. Schwarz, G. Madsen, D. Kvasnicka, J. Luitz, Wien2k, (2001).

[2] J.P. Perdew, K. Burke, M. Ernzerhof, Generalized Gradient Approximation Made Simple, Phys. Rev. Lett. 77 (1996) 3865–3868. https://doi.org/10.1103/physrevlett.77.3865.

[3] A.D. Becke, E.R. Johnson, A simple effective potential for exchange, J. Chem. Phys. 124 (2006) 221101. https://doi.org/10.1063/1.2213970.

[4] V.L. A. Otero-de-la-Roza, D. Abbasi-Pérez, Gibbs2: A new version of the quasiharmonic model code. II. Models for solid-state thermodynamics, features and implementation, Comput. Phys. Commun. 182(10) (2011) 2232–2248.

[5] V.L. A. Otero-de-la-Roza, Gibbs2: A new version of the quasi-harmonic model code. I. Robust treatment of the static data, Comput. Phys. Commun. 182(8) (2011) 1708–1720.

[6] F.D. Murnaghan, The compressibility of media under extreme pressures, Proc. Natl. Acad. Sci. U. S. A. 30 (1944) 244.

[7] S.S. Essaoud, A.S. Jbara, First-principles calculation of magnetic, structural, dynamic, electronic, elastic, thermodynamic and thermoelectric properties of Co2ZrZ (Z= Al, Si) Heusler alloys, J. Magn. Magn. Mater. (2021) 167984.

[8] P.L. Dulong, A.-T. Petit, Recherches sur quelques points importans de la theorie de la Chaleur, 1819.

[9] M. Jamal, S. Jalali Asadabadi, I. Ahmad, H.A. Rahnamaye Aliabad, Elastic constants of cubic crystals, Comput. Mater. Sci. 95 (2014) 592–599. https://doi.org/10.1016/j.commatsci.2014.08.027.

[10] I.R. Shein, A.L. Ivanovskii, Elastic properties of superconducting MAX phases from first-principles calculations, Phys. Status Solidi B 248 (2011) 228–232.

[11] M. Born, K. Huang, Theory of Crystal Lattices, Clarendon, Oxford, 1956.

[12] M.F. Cover, O. Warschkow, M.M.M. Bilek, D.R. McKenzie, A comprehensive survey of M2AX phase elastic properties, J. Phys. Condens. Matter 21 (2009) 305403.

[13] G. Surucu, A. Candan, A. Gencer, M. Isik, First-principle investigation for the hydrogen storage properties of NaXH3 (X= Mn, Fe, Co) perovskite type hydrides, Int. J. Hydrog. Energy 44 (2019) 30218–30225.

[14] S.N. Tripathi, V. Srivastava, S.P. Sanyal, First Principle Mechanical and Thermodynamic Properties of Some TbX (X= S, Se) Compounds, J. Supercond. Nov. Magn. 32 (2019) 2931–2938.

[15] S.N. Tripathi, V. Srivastava, H. Pawar, S.P. Sanyal, First-principles investigation of structural, electronic and mechanical properties of some Dysprosium chalcogenides, DyX (X= S, Se and Te), Indian J. Phys. 94 (2020) 1195–1201.

CONCLUSION

Conclusion

Our analysis in this work involved a thorough verification of the properties of V_2SnC and V_2SnN, from which we obtained the following results:

- Both V_2SnC and V_2SnN share a hexagonal crystal structure ($P6_3/mmc$ space group) and exhibit metallic behavior due to overlapping valence and conduction bands.
- V_2SnC generally shows higher mechanical resistance (larger lattice constant, bulk modulus, and stiffness) compared to V_2SnN, which is softer and more machinable.
- Electronic contributions differ: V_2SnN primarily involves V-d and N-p orbitals, while V_2SnC involves C-p and V-d orbitals. Bonding analysis suggests predominantly ionic bonding for both (more so in V_2SnN), with V_2SnC showing more covalent character and V_2SnN more metallic character.
- Both compounds display anisotropic behavior.
- Their thermodynamic properties (heat capacity, entropy, thermal expansion coefficient, and Debye temperature) were studied, showing expected trends with temperature and pressure. For instance, heat capacity follows the Dulong–Petit law at high temperatures and decreases with pressure, while entropy increases with temperature and decreases with pressure.
- Mechanical stability for both compounds is confirmed by calculated elastic constants meeting Born-Huang criteria.

ملخص

فـي عملنـا هـذا قمنـا بدراسـة نظريـة لحسـاب الخـواص البنيويـة ، الالكترونيـة ، المرونيـة والترموديناميكية للمركبين V_2SnC وV_2SnN وذلك باستعمال تقريب التدرج المعمم GGA-PBEsolالمعتمدة على نظرية دالية الكثافة (DFT) ، فيما يخص الخواص البنيوية قمنا بحساب ثابت الشبكة ، معامل الانظغاطية ، والمشتقة الأولى له بالنسبة للضغط ، ولفهم السلوك الالكتروني لكلا المركبين قمنا بتحليل بنية عصابات الطاقة الإلكترونية وأطياف الكثافة الحالات الإلكترونية DOS الكلية و الجزئية .بعد ذلك، تم تقييم الخواص المرنة من خلال حساب الثوابت المرنة الأساسية ، بالإضافة إلى المعاملات المشتقة مثل معامل القص، معامل يونغ، ونسبة بواسون و في الاخير قمنا بدراسة الخواص الحرارية، بما في ذلك السعة الحرارية، الإنتروبيا، معامل التمدد الحراري، درجة حرارة ديباي، ومعامل الانضغاطية تحت تأثير درجات حرارة وضغوط مختلفة.

Abstract

In this work, we carried out a theoretical study to investigate the structural, electronic, elastic, and thermodynamic properties of the compounds V2SnC and V2SnN using the GGA-PBEsol approximation within the framework of Density Functional Theory (DFT). For the structural properties, we calculated the lattice constants, bulk modulus, and its first pressure derivative. To understand the electronic behavior of both compounds, we analyzed the electronic band structure and the total and partial density of states (DOS). Subsequently, the elastic properties were evaluated by calculating the fundamental elastic constants, along with derived parameters such as the shear modulus, Young's modulus, and Poisson's ratio.

Finally, the thermodynamic properties were studied, including heat capacity, entropy, thermal expansion coefficient, Debye temperature, and bulk modulus under varying temperature and pressure conditions.